



## RESEARCH ARTICLE

10.1029/2024MS004307

## Key Points:

- A novel process-based SED model is developed for applications with coarse spatial and temporal resolutions of precipitation
- The SED model is coupled with VIC accounting for subgrid-scale variability of rainfall intensity, soil, vegetation, and flow path length
- The coupled VIC-SED model is evaluated with two case studies and its model parameters are insensitive to spatial and temporal resolutions

## Correspondence to:

X. Xie and X. Liang,  
xianhong@bnu.edu.cn;  
xuliang@pitt.edu

## Citation:

Xie, X., & Liang, X. (2024). Coupling soil erosion and sediment transport processes with the Variable Infiltration Capacity model (VIC-SED) for applications suitable with coarse spatial and temporal resolutions. *Journal of Advances in Modeling Earth Systems*, 16, e2024MS004307. <https://doi.org/10.1029/2024MS004307>

Received 25 FEB 2024  
Accepted 26 AUG 2024

# Coupling Soil Erosion and Sediment Transport Processes With the Variable Infiltration Capacity Model (VIC-SED) for Applications Suitable With Coarse Spatial and Temporal Resolutions

Xianhong Xie<sup>1,2</sup>  and Xu Liang<sup>2</sup> 

<sup>1</sup>State Key Laboratory of Remote Sensing Science, Faculty of Geographical Science, Beijing Normal University, Beijing, China, <sup>2</sup>Department of Civil and Environmental Engineering, University of Pittsburgh, Pittsburgh, PA, USA

**Abstract** Understanding soil erosion and sediment transport from the hillslope scale to the regional scale is crucial for studies on water quality, soil-water conservation, the lateral carbon cycle, environmental zoning and vulnerability. However, most existing erosion and sediment transport models are only applicable at the hillslope scale or for small watersheds with fine spatial resolutions (typically much less than 1 km). This study presents a process-based soil erosion and sediment transport model for model applications designed for applications with coarse spatial (e.g.,  $\geq 10$  km) and temporal (e.g., from hourly to daily) resolutions. This new model, referred to as VIC-SED, effectively accounts for interactions between erosion and hydrological processes. This is achieved by tightly coupling the erosion processes with a hydrologically based Three-layer Variable Infiltration Capacity (VIC-3L) land surface model (LSM) and to a multi-scale routing (MSR) model. VIC-SED considers the impacts of (a) the spatio-temporal variability of rainfall intensity on erosion processes and (b) soil moisture on the soil detachment process. VIC-SED is evaluated in two watersheds. Results demonstrate that VIC-SED is capable of reproducing water and suspended sediment discharges at coarse spatial resolutions and varying temporal scales varying from 15-min to daily intervals. Our study indicates that the VIC-SED model is a promising tool for studying and assessing the impacts of climate and land cover changes on suspended sediment yields over large regions using coarse spatial and temporal resolutions.

**Plain Language Summary** Soil erosion is a global issue impacting soil-water conservation, making the qualification of sediment transport crucial for evaluating water quality and landscape evolution. Existing models predominantly focus on hillslopes or small watersheds, with limited applicability to larger spatial scales. This limitation is partly due to the complexity of erosion processes and the empirical formulations involved in the erosion and sediment transport. To address this gap, we developed a novel process-based soil erosion and sediment transport model for large-scale land surface modeling. This model is integrated with the sophisticated Three-layer Variable Infiltration Capacity (VIC-3L) hydrological model and a multi-scale routing (MSR) scheme for water and sediment transport. It explicitly accounts for the spatial and temporal variability of rainfall intensity and formulates the impact of soil moisture on the soil detachment process. Results from two applications demonstrate the model's capability to predict soil erosion and sediment dynamics at large spatial and temporal scales.

## 1. Introduction

It is important to adequately estimate soil erosion and suspended sediment discharges at large scales in order to address a wide range of problems, such as impoverishment of the hillslope soil resource, river channel and reservoir siltation, amount of sediment discharged to ocean, water quality, etc., that are crucial for the study of agricultural sustainability, environment health, and climate change impacts (Latocha et al., 2016; Yu et al., 2017). Spatial and temporal information on soil erosion and sediment yield provides particularly useful perspective on the pace of landscape evolution, water quality, and the impact of agricultural practices, lateral carbon accounting, deforestation and other land use changes (e.g., Abaci & Papanicolaou, 2009; Zhang et al., 2020). Moreover, to explore how climate change, especially the seasonal rainfall variability, affects soil erosion, sediment transport and deposition, a better understanding of the relationship between climatic factors and land surface properties at large scales is necessary (Istanbulluoglu & Bras, 2006; Xie et al., 2015). Therefore, it is crucial to have an erosion

© 2024 The Author(s). Journal of Advances in Modeling Earth Systems published by Wiley Periodicals LLC on behalf of American Geophysical Union. This is an open access article under the terms of the [Creative Commons Attribution-NonCommercial-NoDerivs License](https://creativecommons.org/licenses/by/4.0/), which permits use and distribution in any medium, provided the original work is properly cited, the use is non-commercial and no modifications or adaptations are made.

and sediment transport model that allows for having coarse spatial and temporal resolutions to facilitate large scale studies related to these challenging issues (Mao et al., 2010; Stewart et al., 2017).

To the best of our knowledge, there is few such a soil erosion and sediment transport model (called SED model hereafter) yet available using coarse spatial and temporal resolutions. This is because with a coarse resolution (both in space and time), the rainfall intensity, which is typically taken as an average over the modeling grid and time step, would be significantly reduced. Thus, the erosion process (e.g., soil detachment) and sediment transport cannot be adequately represented at the coarse resolution since most of the equations for the erosion processes have been developed with fine resolutions (both in space and time) where intense rainfall intensity plays an important role. Therefore, these equations cannot be directly employed to the coarse resolutions; otherwise, large errors for the soil detachment process would be resulted. In this study, we demonstrate how to overcome such a challenge.

Since the processes of erosion and sediment transport are affected by hydrological processes, a SED model is either tightly coupled to a hydrological model or has the hydrological processes directly included. Therefore, based on the erosion and sediment processes, SED models can be classified into two categories: (a) those suitable for large scale studies using coarse modeling resolutions (e.g.,  $\geq 10$  km in space), and (b) those suitable for small scale studies using fine modeling resolutions (e.g.,  $\leq 500$  m in space). Thus, a model applied to a large-scale study using fine resolution is not considered to be in category 1. For each category, the SED models can be further classified into three groups: empirical, conceptual, and process-based (Merritt et al., 2003). For detail information about the currently available and widely used SED models, such as Universal Soil Loss Equation (USLE), a modified version of USLE (i.e., MUSLE), Water Erosion Prediction Project (WEPP), and European Soil Erosion Model (EUROSEM), readers are referred to the comprehensive reviews (e.g., Aksoy & Kavvas, 2005; de Vente & Poesen, 2005; P. F. Li et al., 2017; Merritt et al., 2003; Stewart et al., 2017; Tan et al., 2018).

The widely used SED models have simplified representations of hydrological processes. For example, the EUROSEM model only considers the surface runoff due to the infiltration excess runoff but not the saturation excess runoff (Baets et al., 2008; Morgan et al., 1998). The Soil and Water Assessment Tool (SWAT) model uses a conceptual curve number to represent the runoff generation (Arnold et al., 1993, 1999, 2012). Other examples include the GIS-based distributed model for soil erosion and sediment yields by Jain et al. (2005) which only considers the infiltration excess runoff as well. The process-based distributed model developed by Kabir et al. (2011) for watershed-scale sediment dynamics only simulates the flood event using a constant runoff coefficient. Although Pelletier (2012) proposed a spatially distributed long-term suspended sediment discharge prediction model for global applications, the model does not include an explicit hydrological parameterization for the daily or sub-daily sediment simulations. It only simulates the monthly average sediment yield. As pointed out by Post et al. (2007), it is essential to couple a sophisticated hydrological model to these SED models which have simplified representations of hydrological processes to fill in the gaps and to better represent the temporal dynamics of the hydrological processes to improve simulations of the erosion and sediment yield processes in the SED models, especially for large scale application studies with these SED models.

In summary, the currently available SED models have at least two main limitations. First, they are developed based on theories and/or findings feasible only for fine spatial and/or temporal resolutions, and thus are usually suitable only for small scale studies. Even though some of these models (e.g., GeoWEPP) have been applied to study large watersheds (Flanagan et al., 2013; Maalim et al., 2013; Miller et al., 2012), the spatial resolutions to which these models are applied were small (e.g.,  $\leq 500$  m). Second, they do not have adequate representations on hydrological processes.

To circumvent these limitations, we present a new SED model which has two distinguished features: (a) allowing coarse spatial and large temporal resolutions as a model computational unit, and (b) having hydrological processes reasonably represented by coupling the erosion and sediment processes to a hydrologically based land surface model (LSM). To address the first limitation, we take a statistical distribution approach to represent the rainfall intensity over a coarse resolution both in space and time. To address the second limitation, we couple the SED related processes to a hydrologically based LSM so that the main and important hydrological processes are adequately represented at a compatible scale. To this end, we employ the Three-layer Variable Infiltration Capacity (VIC-3L) LSM (Liang et al., 1994, 1999, 2003; Liang, Lettenmaier, & Wood, 1996; Liang, Wood, & Lettenmaier, 1996; Liang & Xie, 2001). In this paper, we refer our new SED model to as VIC-SED hereafter. Section 2.2 provides a brief summary of the VIC-3L model to justify its selection. We note that Mao et al. (2010)

connected a soil erosion model with VIC, but it was a one-way coupling in which the VIC output was used as input to drive its soil erosion processes. Therefore, their model cannot represent the feedback effects between the hydrological processes and soil erosion processes. In contrast, VIC-SED is a two-way coupled model.

The remainder of this paper is organized as follows: methodology of the new VIC-SED is presented in Section 2. Section 3 provides the evaluation of VIC-SED in two watersheds. Section 3.1 applies VIC-SED to a small watershed in which impacts of the different temporal resolutions, especially the large temporal resolutions, are investigated while the spatial resolution is kept small. Section 3.2 applies VIC-SED to a large watershed in which impacts of the different spatial resolutions, especially coarse resolutions, are investigated while the temporal resolution is fixed at a large daily time step. Parameter sensitivity analysis is presented in Section 4. Section 5 provides conclusions and future work.

## 2. Methodology

### 2.1. Soil Detachment

This subsection describes how the rainfall kinetic energy is extended from its expressions developed for fine resolutions in both space and time to be suitable for models using coarse resolutions as well. For the soil detachment process, we have also extended some of its primary equations developed in the EUROSEM model (Morgan et al., 1998) for a fine resolution to be applicable to coarse resolutions.

#### 2.1.1. Rainfall Energy Representation

Rainfall kinetic energy is one of the active erosive agents delivered by raindrop during a storm event. It is closely linked to the rainfall type and intensity (Bryan, 2000). Two types of rainfall kinetic energy are typically considered: direct rainfall impact and leaf drip impact. The rainfall energy reaching the land surface as direct throughfall for a point scale is expressed as a logarithmic function of rainfall intensity derived by Brandt (1989). A brief description of the rainfall kinetic energy formulations is provided in Appendix A.

The equations in Brandt (1989, 1990) provide a good point estimation of the rainfall energy. They can be easily applied to a small study area with a short time step since in such a case the averaged areal-temporal rainfall intensity could be a good approximation of the point rainfall intensity,  $r_{i,t}$ . But if one directly applies them to a study area with a coarse modeling resolution, the rainfall energy induced erosion would be significantly underestimated because of the use of averaged areal-temporal rainfall intensity to replace the point rainfall intensity in those original equations. To make the equations also applicable to studies using coarse spatial and temporal resolutions, it is necessary to consider impacts of the subgrid spatial and sub-time temporal variability of the rainfall intensity on the erosion process related to the rainfall kinetic energy. To this end, we employ statistical distributions to describe the rainfall intensity in space and time which has been shown to be effective in previous studies (Liang et al., 2003, 2004; Liang, Lettenmaier, & Wood, 1996; Liang & Xie, 2001; Wen et al., 2012).

To represent the spatial variability of rainfall, a number of distributions have been proposed in the literature, such as the lognormal, gamma, exponential, and weibull distributions (Kundu & Siddani, 2007). As there is no clear evidence regarding which distribution is always significantly better than others (Cho et al., 2004), we employ the lognormal distribution to depict the point rainfall intensity over a large study area. The probability density distribution (PDF) of a point rainfall intensity,  $f_s(r_{i,t})$ , over an area,  $\Delta A$ , at each time  $t$  is expressed as,

$$f_s(r_{i,t}) = \frac{1}{r_{i,t}\sigma_t\sqrt{2\pi}} \exp\left[-\frac{(\ln r_{i,t} - \lambda_t)^2}{2\sigma_t^2}\right] \quad (1)$$

where  $\lambda_t$  and  $\sigma_t$ , respectively, are the mean and standard deviation of the rainfall intensity's natural logarithms over the area at time  $t$ . With such a PDF, the probability of rainfall intensity within  $[r_{i,t}, r_{i,t} + dr_{i,t}]$  stands for the fraction of the study area with rainfall intensity of  $r_{i,t}$ . Thus, combine Equation 1 and Equation A1 in Appendix A, the area-averaged rainfall energy over the study area corresponding to an instantaneous time  $t$ , can be written as,

$$\begin{aligned}
 KE_{DT,s}(t) &= \int_0^{+\infty} KE_{DT,\text{point}}(r_{i,t}) \cdot f(r_{i,t}) dr_{i,t} \\
 &= \int_0^{+\infty} (8.95 + 3.67 \ln r_{i,t}) \cdot \frac{1}{r_{i,t} \sigma_t \sqrt{2\pi}} \exp\left[-\frac{(\ln r_{i,t} - \lambda_t)^2}{2\sigma_t^2}\right] \cdot dr_{i,t} \\
 &= 8.95 + 3.67 \lambda_t
 \end{aligned} \tag{2}$$

The parameters  $\lambda_t$  and  $\sigma_t$  can be estimated in general based on rainfall data at time  $t$ . However, one does not need to estimate  $\sigma_t$  in this case since the variance,  $\sigma_t$ , can be approximated by the sample mean of  $r_{i,t}$  as discussed below. First, the area-averaged rainfall energy,  $KE_{DT,s}(t)$ , can be estimated based on  $\lambda_t$  as follows,

$$\lambda_t = \ln[\bar{r}_t] - \frac{1}{2} \ln\left[1 + \frac{\text{var}(r_{i,t})}{(\bar{r}_t)^2}\right] \tag{3}$$

where  $\bar{r}_t$  (e.g., with a unit mm/h) and  $\text{var}(r_{i,t})$  are, respectively, the expectation of rainfall intensity,  $r_{i,t}$ , and its variance over the area at time  $t$ . Both of them can be approximated with the sample mean and sample variance if enough rainfall gauges are available in the study area of interest. Second,  $\text{var}(r_{i,t})$  can be simplified to be proportional to the square of  $\bar{r}_t$  as follows:

$$\text{var}(r_{i,t}) = \left(\frac{1}{k_r^2} - 1\right) \cdot (\bar{r}_t)^2 \tag{4}$$

where  $k_r$  is a constant parameter between zero and one and is used to characterize the spatial variability of rainfall intensity. The minimum of  $k_r$  is prescribed to be a small value in simulations, for example, 0.01. As  $k_r$  increases, the spatial variability of rainfall intensity decreases.

Thus Equation 2 becomes,

$$KE_{DT,s}(t) = 8.95 + 3.67 \cdot \ln(k_r \cdot \bar{r}_t) \tag{5}$$

Similar to the consideration of the spatial subgrid variability, the sub-time variability of rainfall within a large time step,  $\Delta t$ , also needs to be taken into account. In our approach, we assume the expectation of areal rainfall intensity (i.e.,  $\bar{r}_t$ ) is independent of its temporal variability (Rodríguez-Iturbe & Mejía, 1974). For the temporal variability, we use a simple exponential rainfall depth-intensity distribution (ERDID) proposed by van Dijk et al. (2005), which has been evaluated and also successfully applied to the runoff and erosion studies using the Revised Universal Soil Loss Equation (RUSLE) and the Griffith University Erosion System Template (GUEST) approaches. Based on this ERDID approach, the probability density function of the areal-average rainfall depth over a storm duration,  $\Delta t$ , can be expressed as,

$$f_t(\bar{r}_t) = \frac{1}{\bar{r}'} \exp\left(-\frac{\bar{r}_t}{\bar{r}'}\right) \tag{6A}$$

$$\bar{r}' = \frac{\int_0^T (\bar{r}_t)^2 \cdot dt}{\int_0^T \bar{r}_t \cdot dt} \tag{6B}$$

where  $\bar{r}'$  is the depth-averaged rainfall intensity of a storm,  $T$  is the duration of a storm or approximated by the storm mean rainfall intensity over a study area. Note that the probability of the rainfall depth over  $[\bar{r}_t, \bar{r}_t + d\bar{r}_t]$ , defined by Equation 6A, represents the fraction of the entire storm duration with rainfall depth of  $\bar{r}_t$ . An advantage of using a probability distribution is that information about the fine rainfall intensity series over the storm duration is no longer needed.

Thus, the average rainfall energy for an area  $A$  with a storm duration of  $T$  can be expressed as,

$$\begin{aligned}
 KE_{DT} &= \int_0^{+\infty} KE_{DT,s}(t) \cdot f_i(\bar{r}_i) \cdot d\bar{r}_i = \int_0^{+\infty} [8.95 + 3.67 \cdot \ln(k_r \cdot \bar{r}_i)] \cdot \frac{1}{\bar{r}} \exp\left(-\frac{\bar{r}_i}{\bar{r}}\right) \cdot d\bar{r}_i \\
 &= 8.95 + 3.67 \ln k_r + \frac{3.67}{\bar{r}} \cdot \int_0^{+\infty} (\ln \bar{r}_i) \cdot \exp\left(-\frac{\bar{r}_i}{\bar{r}}\right) d\bar{r}_i
 \end{aligned} \tag{7}$$

where the integration term in Equation 7 is solved using a numerical integration algorithm, such as the Simpson integration. Replacing the point-scale total kinetic energy (i.e.,  $KE_{DT,point}$  in Equation A3) by Equation 7, we can get the total rainfall energy,  $KE$ , for an area  $\Delta A$  with a storm duration  $T$  as follows,

$$KE = KE_{DT} \cdot (1 - f_c) \cdot R_{Total} + KE_{LD} \cdot f_c \cdot R_{Net} \tag{8}$$

Except for  $KE_{DT}$ , meanings of other terms in Equation 8 are defined and explained in Equations A2–A4 in Appendix A. If we replace the area  $\Delta A$  by a modeling grid cell and the storm duration  $T$  by a modeling time step,  $\Delta t$ , then Equation 8 can be used to represent the total rainfall energy applicable to large scale studies with a coarse resolution in space and time. As we know for large scale studies, the spatial resolution of a modeling grid size is typically on the order of kilometers, (e.g.,  $\geq 1$  km), and the temporal resolution varies from hourly to daily or even longer. These resolutions are much larger than the resolutions where Equations A1 and A3 are suitable for, which are for scales on an order of meters in space and minutes in time. Therefore, if we still applied Equations A1 and A3 to studies with coarse spatial and temporal resolutions, large errors would be resulted, although such large errors were usually compensated through estimated model parameters.

### 2.1.2. Detachment by Raindrop Impact

Torri et al. (1987) proposed a linear relationship between soil detachment and rainfall energy, combined with the effect of surface water (runoff) depth. This effect is well quantified by Parks et al. (1982) as applied in Kabir et al. (2011). In this study, we employ the relationship presented by Torri et al. (1987) and Parks et al. (1982), and add an adjustment factor to the detachment equation to represent the soil moisture effect, because soil moisture is one of the most active factors impacting the erosion process (Bryan, 2000). Thus slightly modified soil detachment for an area can be expressed as,

$$DR = \frac{k_b F_h F_\theta}{\rho_s} \cdot KE \tag{9}$$

where  $DR$  is the soil detachment due to rain drops during a time step ( $L^3/L^2/T$ ),  $\rho_s$  is the particle density ( $M/L^3$ ),  $k_b$  represents the maximum detachability when the soil is at the saturation state ( $M/W$ ),  $F_h$  is a factor accounting for water ponding effect which is described in Appendix B.  $F_\theta$  is an adjustment factor we introduced in this study to account for the response of soil strength to soil water content.  $KE$  is the kinetic energy described in Equation 8 ( $W/L^2$ ). It is worth mentioning that there are two main differences between Equation 9 and the relationship presented by Torri et al. (1987) and Parks et al. (1982). The first is that the kinetic energy,  $KE$ , in this equation is no longer required to be computed based on using fine spatial and temporal resolutions. Second is the introduction of impact of soil moisture through  $F_\theta$ .

Although the response of soil strength to soil moisture is complex, the cohesive strength of most soil types appears to show a similar pattern: the cohesive strength declines with the increase of soil water content (Bryan, 2000). For example, the WEPP model (Flanagan & Nearing, 1995; Laflen et al., 1991) uses an exponential equation to depict the factor of sealing and crusting with a time variable, the cumulative days after soil disturbance (e.g., tillage, irrigation). Motivated by their formulation, we proposed a new exponential equation with the adjustment factor for soil water content, which is as follows,

$$F_\theta = \exp\left[a \cdot \frac{\theta}{\theta_{sat}}\right] \tag{10}$$

where  $\theta$  and  $\theta_{\text{sat}}$  are soil water and saturated soil water contents ( $L^3/L^3$ ),  $a$  is a parameter used to characterize impacts associated with the soil intrinsic properties such as clay, organic matter and oxides contents. Such properties significantly contribute to the cohesive strength of aggregates and influence the splash detachment (Wuddivira et al., 2009). For coarse-resolution modeling, we suggest that this parameter,  $a$ , be determined through a model calibration process. For fine-resolution studies, this parameter,  $a$ , can be determined through experiments at a plot scale.

As can be seen, the factor,  $F_{\theta}$ , increases with the increase of  $\theta$ , implying an increase of soil detachment due to the soil moisture status. During a non-rainfall period, the soil detachability decreases as the soil moisture is consumed by evapotranspiration. This description of the behavior of the soil detachability is consistent with the concept used in the WEPP model in its representation of the sealing and crusting impact after soil disturbance (Flanagan & Nearing, 1995). Thus Equation 10 explicitly considers the partial impact of the soil moisture content on the soil detachment process. This work explicitly accounts for the impact of rainfall heterogeneity on the estimate of the rainfall energy,  $KE_{DT}$ , while impacts of the other heterogeneities (such as soil properties, vegetation, etc.) on the detachment process are only indirectly considered through their impacts to the soil moisture represented by the VIC-3L hydrological model.

### 2.1.3. Detachment by Overland Flow

Soil erosion by overland flow and the sediment deposition are two counteracting processes. Smith et al. (1995) described the balance between these two processes by representing the transport capacity concentration of runoff. Their approach was adopted in the EUROSEM model (Morgan et al., 1998) and here as well. Specifically, the net runoff detachment is expressed as (Morgan et al., 1998; Smith et al., 1995),

$$DF = \beta \omega_s (TC - C) \quad (11)$$

$$\beta = \begin{cases} 0.79 \cdot \exp(-0.85 \cdot J), J \geq 1 \\ 1, J < 1 \end{cases} \quad (12)$$

where  $DF$  is the net detachment of soil particles by the flow ( $L^3/L^2/T$ ) during a time step,  $\beta$  is a flow detachment efficiency coefficient, a function of the cohesion of the soil  $J$  (W/P) which is strongly impacted by soil moisture,  $\omega_s$  is the particle settling velocity ( $L/T$ ),  $TC$  is the transport capacity concentration ( $L^3/L^3$ ), and  $C$  is sediment concentration ( $L^3/L^3$ ). The sediment deposition occurs when  $DF$  is negative ( $TC < C$ ). Their formulations for the settling velocity ( $\omega_s$ ) and the transport capacity concentration ( $TC$ ) are briefly presented in Appendix C.

In Equation 12 the cohesion ( $J$ ) is an input parameter that needs to be measured in the field. While it may be feasible for an event-based erosion model, such as EUROSEM, to measure such cohesive strength before a simulation is carried out, such required measurement information is not applicable for a continuous model. Since the cohesive strength is inversely linked to water content except at very low water contents (Bryan, 2000), many researchers have proposed both theoretical and empirical formulations to estimate the relationship between the soil water content and shear strength (Fredlund et al., 1995). But most of their formulations employ parameters that are difficult to prescribe for a coarse-resolution modeling. Mouazen et al. (2002) established an empirical regression equation for soil shear strength, bulk density and moisture content. In the equation, the soil cohesion is a linear function of the soil moisture for sandy loam soil. Matsushi and Matsukura (2006) proposed an exponential function to express the relationship between the cohesion and soil moisture content. Although the function lacks theoretical validity from a physical standpoint of view, the parameters involved in the function can be obtained by experiments or through a model calibration process. Hence, we use their proposed empirical relationship to estimate the soil cohesion. The expression is as follows,

$$J = J_{\text{max}} \exp\left(-\mu \cdot \frac{\theta}{\theta_{\text{sat}}}\right) \quad (13)$$

where  $J$  is the estimated cohesion,  $J_{\text{max}}$  is the hypothetical maximum value of cohesion (when  $\theta = 0$ ),  $\mu$  is a coefficient related to susceptibility of the shear strength to the soil moisture impact ( $\mu > 0$ ). The parameters  $J_{\text{max}}$  and  $\mu$  can be prescribed by the procedure proposed in Matsushi and Matsukura (2006) or by model calibration.

Again, it should be noted that impacts of the heterogeneities of soil and vegetation properties on  $DF$  are generally not accounted for in most of such models due to the limitation of required information. However, such impacts can be partially represented through the soil moisture  $\theta$  in Equation 13 if the estimate of  $\theta$  from a hydrological model/LSM accounts for the effects of soil and vegetation heterogeneity, similarly to how the heterogeneity's impact is considered in  $F_\theta$  (i.e., Equation 10).

## 2.2. Integration of Soil Detachment Process With Hydrological Processes

As can be seen from Section 2.1, certain hydrological variables, such as soil moisture and surface runoff, are needed in computing the soil detachment through  $DR$  and  $DF$ . Moreover, to have the expressions of Equation 9 for  $DR$  and Equation 11 for  $DF$  more applicable to coarse-resolution studies, it is important that these hydrological variables are estimated by considering the impact of subgrid variability (e.g., soil properties, vegetation, etc.). To achieve this, we select the hydrologically based land surface model, the VIC-3L model (Liang, Lettenmaier, & Wood, 1996; Liang, Wood, & Lettenmaier, 1996; Liang & Xie, 2001; Liang et al., 1994, 1999, 2003), and have it coupled with the soil detachment processes. VIC-3L is selected due to its distinguished features: (a) representation of subgrid spatial variabilities of soil properties and precipitation; (b) accounting for both infiltration and saturation excess runoff generation mechanisms inactively under the context of subgrid spatial variabilities; (c) representation of the dynamic interactions between surface and groundwater and the impact of such interactions on surface fluxes and soil moisture state (Leung et al., 2010); (d) simulation of snow and frozen soil processes for cold climate conditions, and (e) explicit characterization of multiple land cover types and a simple yet reasonable representation of ground heat fluxes both for bare and vegetated surfaces (Liang et al., 1999). Also, VIC-3L has been extensively tested and successfully applied to numerous studies at multiple scales from watershed (e.g., Liang & Xie, 2001), to regional (e.g., Maurer et al., 2002), and to global scale (e.g., Nijssen et al., 2001). For details of the VIC-3L model and its previous versions, the reader is referred to (Cherkauer & Lettenmaier, 1999; Huang & Liang, 2006; Liang, Lettenmaier, & Wood, 1996; Liang, Wood, & Lettenmaier, 1996; Liang & Xie, 2001; Liang et al., 1994, 1999, 2003).

For each time step, VIC-3L computes the soil moisture,  $\theta$ , at different soil depth, then, it is used in Equations 10 and 13 to calculate  $F_\theta$  and  $J$ , respectively. Since the soil moisture  $\theta$  estimated from VIC-3L partially accounts for the impact of spatial subgrid heterogeneity due to the precipitation, soil and vegetation, the estimations of both  $F_\theta$  and  $J$  thus partially account for the impacts of subgrid variability through the soil moisture content  $\theta$  and therefore, they are in line with the treatment of the rainfall energy for applications to large scale studies.

## 2.3. Sediment Transport and River Erosion

The sediment transport over land, within rivers, and through river network is described in which the process of river bed erosion is considered. The mass conservations of water and sediment overland and in the channel, in conjunction with the motion of the kinematic wave, can be expressed as follows,

$$\frac{\partial q}{\partial x} + m \cdot \xi \cdot q^{\xi-1} \cdot \frac{\partial q}{\partial t} = R \quad (14)$$

$$\frac{\partial q_{\text{sed}}}{\partial x} + \frac{\partial h_{\text{sed}}}{\partial t} - e(x, t) = R_{\text{sed}} \quad (15)$$

$$q_{\text{sed}} = q \cdot C_{\text{sed}}, h_{\text{sed}} = m \cdot q^\xi \cdot C_{\text{sed}}, m = \left( \frac{n}{\sqrt{S}} \right)^\xi \quad (16)$$

where  $q$  is the unit-width flow ( $L^3/L/T$ ),  $R$  is either the surface runoff ( $L/T$ ) generated by the VIC-3L model for the modeling grid cell or the lateral flow from adjacent modeling grid cells and can be estimated from the routing process,  $q_{\text{sed}}$  is the unit-width sediment flow ( $L^3/L/T$ ),  $C_{\text{sed}}$  is the suspended sediment concentration ( $L^3/L^3$ ),  $\xi$  takes the value of 3/5 derived from the Manning's equation,  $n$  is the Manning coefficient and  $S$  is the slope of the hydraulic grade line or the channel bed slope when water depth is or approximated as a constant.  $e(x, t)$  is the net detachment rate over hillslope or the net erosion rate of river channel ( $L^3/L^2/T$ ).  $R_{\text{sed}}$  is the lateral sediment flow ( $L^3/L^2/T$ ) from adjacent modeling grid cells and is computed from the overland flow routing process.

For the hillslope erosion,

$$e(x, t)_{hs} = DR + DF \quad (17)$$

where  $e(x, t)_{hs}$  is the erosion rate on the hillslope,  $DR$  is the soil detachment by rain drops, computed by Equation 9, and  $DF$  is the soil detachment by overland flow, computed by Equation 11.

The channel erosion and sediment deposition processes are simulated using an approach similar to that for the overland flow erosion (i.e., Equation 11), as is done in the EUROSEM model (Morgan et al., 1998). To consider the effect of different types of channel bed loads, a channel erodibility factor ( $K_{ch}$ ) is used to replace the flow detachment efficiency coefficient,  $\beta$ , included in Equation 11. The net erosion rate in channels is then expressed as,

$$e(x, t)_{ch} = k_{ch}\omega_s(TC - C) \quad (18)$$

With this equation, there is no channel erosion ( $e(x, t)_{ch} = 0$ ) when the suspended sediment concentration is greater than or equal to the transport capacity. The channel erodibility factor ( $k_{ch}$ ) is determined by bank and bed stability, depending on factors like the slope of the banks, type of soil or rock, and the presence of vegetation. It can be either measured over a river segment or calibrated through a model calibration process, with its magnitude ranging from 0.0 to 1.0. A higher value indicates greater erosive potential for the channel. The channel erodibility factor is treated similarly to the approach used in the SWAT model (Allen et al., 1999). Despite differences in spatial delineation and hydrological processes treatment on land surface, it is important to note that VIC-SED and SWAT can share channel properties, including erodibility, when formulating sediment transport in river systems.

Equations 14–18 are implemented and solved within the framework of a multiscale routing (MSR) model developed for water by Guo et al. (2004) and improved by Wen et al. (2012) in which the water transport equations are replaced by Equations 14–18. The MSR model employs the kinematic wave method to route both the overland and channel flows. It also assumes a rectangular shape of cross-section area for channels. Main features of the MSR model include: (a) a concept of a tortuosity coefficient—a ratio between the lengths of the river reaches based on the fine digital elevation model (DEM) resolution and the coarse LSM modeling resolution—which is introduced to scale flow velocity, travel time, etc. in order to reduce impacts caused by the large difference between a coarse LSM modeling resolution (e.g., 10 km or larger) and a fine DEM resolution (on an order of meters), (b) allowing the surface runoff generated within a land surface modeling grid cell to simultaneously exit its modeling grid cell through multiple directions, and (c) the use of a statistical distribution/histogram, based on the DEM data, to represent the overland flow path length which reduces impacts of different temporal resolutions on the routing results. Because of these good features, the MSR model has a characteristic of reducing impacts of different resolutions (both in space and time) on the routing results (Wen et al., 2012). Comparing to the D8-based (eight direction based) routing models, whose flow network is generated from the widely used eight direction (D8) method (O'Callaghan & Mark, 1984), results from the MSR model have shown to be significantly less affected by the spatial and temporal resolutions than those from the D8-based routing method (Wen et al., 2012).

The VIC-SED model is an effective integration of the erosion processes and sediment transport processes into the VIC-3L land surface/hydrological model and the MSR routing model. This VIC-SED model is suitable for large scale sediment studies using coarse-resolution due to its consideration of the subgrid variability of rainfall energy in space and time on the detachment process and its conjunctions with the other effective subgrid variability treatments on soil moisture, overland flow path lengths, vegetation, etc. through VIC-3L and MSR. It is important to note, however, that the ideas and processes presented in our SED model for the rainfall energy are general and thus, can be employed in conjunction with other land surface and routing models where impacts of subgrid variability for soil moisture, vegetation, and routing are also considered.

#### 2.4. Model Input and Parameters

The VIC-3L model provides the hydrological components for VIC-SED, so its input and parameters for the water balance simulation are all required to underpin the SED simulations. The input includes meteorological forcing data and values for model parameters which are related to the soil, vegetation, topography and river networks. For details the reader is referred to (Liang, Lettenmaier, & Wood, 1996; Liang & Xie, 2001; Liang et al., 1994; Wen

**Table 1**  
*Primary Parameters Required for the SED Module in the VIC-SED Model*

Parameter	Description (Unit)	Estimation method	Range (Min., Max.)
$k_r$	Parameter for spatial distribution of rainfall intensity (—)	Experiment or Calibration	(0.01, 1.0)
$\alpha$	Coefficient for soil moisture impact on rainfall detachment (—)	Experiment or Calibration	(0.01, 10.0)
$\mu$	Coefficient for soil moisture impact on runoff detachment (—)	Experiment or Calibration	(0.01, 10.0)
$J_{max}$	Maximum soil cohesion (kPa)	Experiment, soil data base or Calibration	(0.01, 50.0)

et al., 2012). There are studies discussing the sensitivity of the VIC-3L parameters (e.g., Demaria et al., 2007; Huang & Liang, 2006; Liang et al., 2003; Liang & Guo, 2003).

Parameters directly related to the SED model component can be divided into two groups. The first group includes parameters (e.g., the rainfall detachability  $K_b$ ) that can be prescribed based on relevant soil databases, for example, the database within the EUROSEM (R. Morgan et al., 1998). The second group contains parameters that need to be calibrated. There are four such parameters in VIC-SED (Table 1). To facilitate the model calibration, ranges for these parameters are provided in Table 1, which are informed by the literature (e.g., Morgan & Nearing, 2011; Neitsch et al., 2011) and are designed to cover a wide array of conditions, as these parameters depend on factors such as soil properties, the size of the study area, and geographical locations. Despite that the default values of both groups of the parameters can be obtained from the relevant soil databases and model parameter databases, we recommend they be calibrated, if possible, due to the coarse spatial resolutions involved in the applications. In this study, the calibration process began with a parameter sensitivity analysis (see Section 4), followed by manual calibration of the identified parameters. Based on the sensitivity analysis, we first calibrated the most sensitive parameters,  $\mu$  and  $J_{max}$ , followed by  $k_r$ , and then the remaining parameters. This calibration order aligns with the principles of the new calibration method demonstrated by Sun et al. (2020), which has shown superior performance. The sensitivity analysis, along with suitable parameter values is detailed in Section 4.

### 3. Results for VIC-SED Evaluation

The VIC-SED model is evaluated at two different watersheds (Figure 1). The first one is a small watershed called Y2, with a drainage area of only 0.534 km<sup>2</sup>, at the Agricultural Research Service (USDA-ARS) Grassland, Soil and Water Research Laboratory near Riesel, Texas. The second one is a large watershed called Big Darby Creek with a drainage area of 2,263 km<sup>2</sup> in Ohio. The purpose of applying VIC-SED to a small watershed is to examine the effectiveness of the model formulations in dealing with coarse temporal resolutions due to the available observations at fine temporal resolutions. The larger watershed is used to test the effectiveness of the VIC-SED formulations in dealing with coarse spatial resolutions. Although evaluations of VIC-SED at the regional or global scales are not conducted in this study, they are indirectly evaluated as one of the challenges in large-scale applications is how to deal with coarse temporal and spatial resolutions. With evaluations on both coarse temporal and spatial resolutions as the first step, we will be able to evaluate VIC-SED at the regional and/or global scales next when the data preparation is completed.

#### 3.1. Application of VIC-SED to a Small Watershed

The small watershed Y2 contains a few good features that facilitate the test of the VIC-SED model. For example, the land cover and the soil distribution are relatively homogeneous (Allen et al., 2005). The breakpoint measurements, including climatic, hydrological and sediment data, are easily accessible. Here, the breakpoint measurements refer to a special type of data whose time and the corresponding magnitude are provided whenever the value of the variable (e.g., rainfall) changes from one steady value to another. Based on these short time-step ( $\Delta t$ ) measurements, event-based simulations can be conducted and used as a benchmark to evaluate our new sediment erosion and transport model which permits the use of a larger time-step,  $\Delta t$ , as its intervals, as opposed to a small time-step that the sediment process requires.

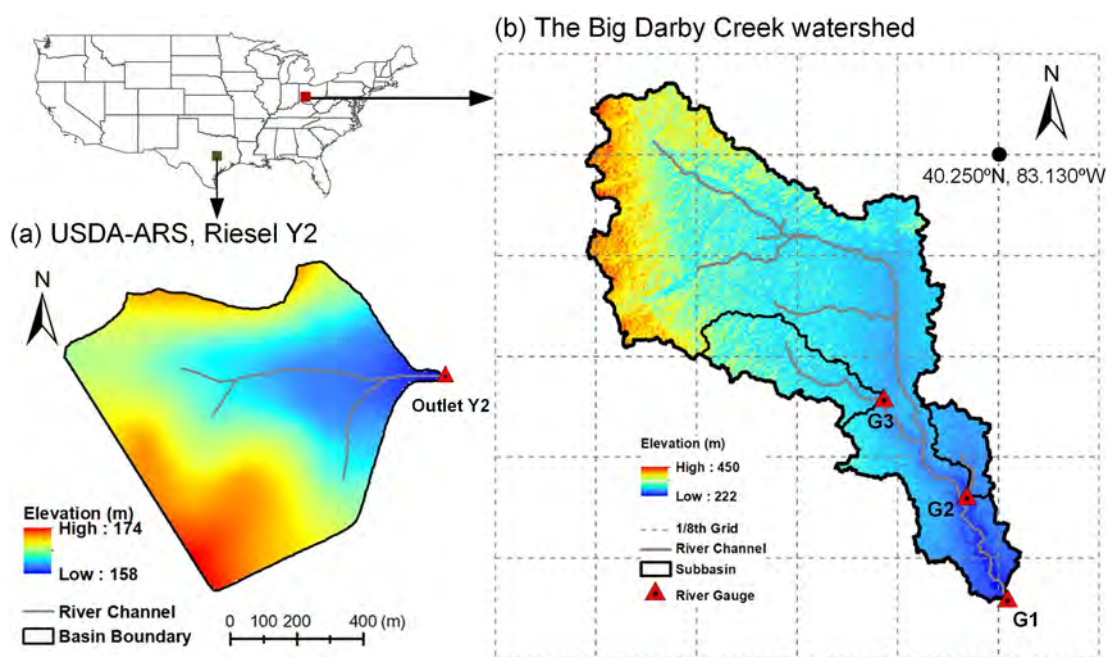


**Figure 1.** Locations and elevation maps of (a) the USDA-ARS Y2 watershed and (b) the watershed of the Big Darby Creek in Ohio. The three streamflow gauges in (b) are G1 (USGS 03230500, 2,263 km<sup>2</sup>), G2 (USGS 03230450, 86 km<sup>2</sup>) and G3 (USGS 03230310, 133 km<sup>2</sup>). The grid cell in (b) has a resolution of 1/8th degree for the VIC-3L modeling.

### 3.1.1. Data Description and Model Setup

The climatic forcing, hydrological and sediment related data sets are all downloaded from the USDA-ARS website (<http://www.ars.usda.gov>). These data sets are associated with three different time scales: breakpoint (2–30 min mostly), hourly and daily time steps. To set a short-event simulation (i.e., with the 15-min time step), the breakpoint data are processed to 15-min regular time interval by using linear interpolation between measurement points. The suspended sediment loading and runoff are corresponding to the outlet of the Y2 watershed. The digital elevation model (DEM) with resolution of 1/3 arc-second (~10 m) from USGS National Elevation Data set (NED) is used to delineate the river channels as shown in Figure 1. There are two types of land cover: cropland (corn, 48.2%) and pasture (52.8%). Monthly LAI values are obtained from the remote sensing retrieval (Maurer et al., 2002). The dominant soil is the Houston Black clay which is prone to shrink and swell with changes of moisture content (Allen et al., 2005; Jeong et al., 2011). Since the Y2 watershed is small with its drainage area less than 1 square kilometer, only one modeling grid cell is used to represent the watershed.

Model simulations were conducted with three different time steps: 15-min, hourly, and daily. For the daily time step simulations, we also performed two additional experiments: one without the representation of temporal variability of rainfall intensity (i.e., Equation 6), and another where model parameters calibrated at daily resolution were applied to hourly simulations. In total, five experiments were conducted to investigate temporal aspects, designated as Exp1, Exp2, Exp3, Exp4, and Exp5.

For Exp1, the model parameters listed in Table 1 were manually calibrated for VIC-SED using an hourly time step. For Exp2 and Exp3, the calibrated model parameters from Exp1 were applied to VIC-SED with 15-min and daily time steps, respectively. In Exp4, the representation of temporal variability of rainfall intensity (i.e., Equation 6) was removed from VIC-SED, while the calibrated model parameters from Exp1 were still applied. For Exp5, we evaluated VIC-SED's performance at finer resolutions using parameters calibrated at coarser resolutions.

These five different experimental settings were used not only to test the formulations of the VIC-SED model on its effectiveness in dealing with the temporal variability of rainfall, but also to demonstrate that this model is adaptable to both event-based simulations and continuous-based long-term simulations. Since this watershed is small, an experiment scenario considering the spatial variability was not needed.

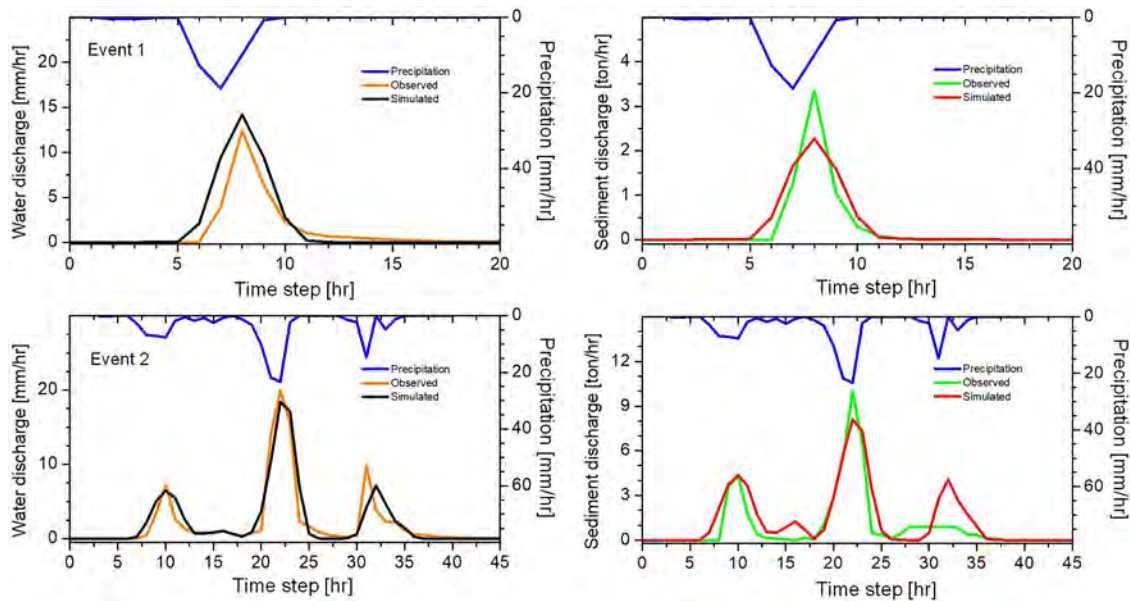


**Figure 2.** Results of Exp1: Hourly water (left) and sediment (right) discharge at the outlet of the Y2 watershed for events 1 and 2 over the calibration period.

All of the five model simulations were conducted for the years of 2001 and 2002 due to the quality of data available, as shown in Jeong et al. (2011). Observed water discharge and sediment discharge at the outlet were used to calibrate and test the model. Due to the limited sediment data—only 15 days in 2001 and 13 days in 2002—we utilized two events from 2001, each lasting over 20 hr (referred to as Event 1 and Event 2), to calibrate the VIC-SED model parameters. Additionally, we tested the VIC-SED model using two events from 2002 (Event 3 and Event 4). For the simulation using a daily time step, we evaluated the simulated suspended sediment based on observations from 28 days, with 15 observations from 2001 to 13 observations from 2002, though the VIC-SED model simulation was conducted throughout the entire year of 2001 and 2002. Note that the model was calibrated using the hourly simulation (Exp1) and tested in the other three simulations in Exp2, Exp3, and Exp4, thus, the values of the model parameters remained the same in the four simulations except for Exp5. Nash-Sutcliffe efficiency (NSE) (Nash & Sutcliffe, 1970), the relative root mean square error (RRMSE), and relative biases were calculated to evaluate the model performance of each case.

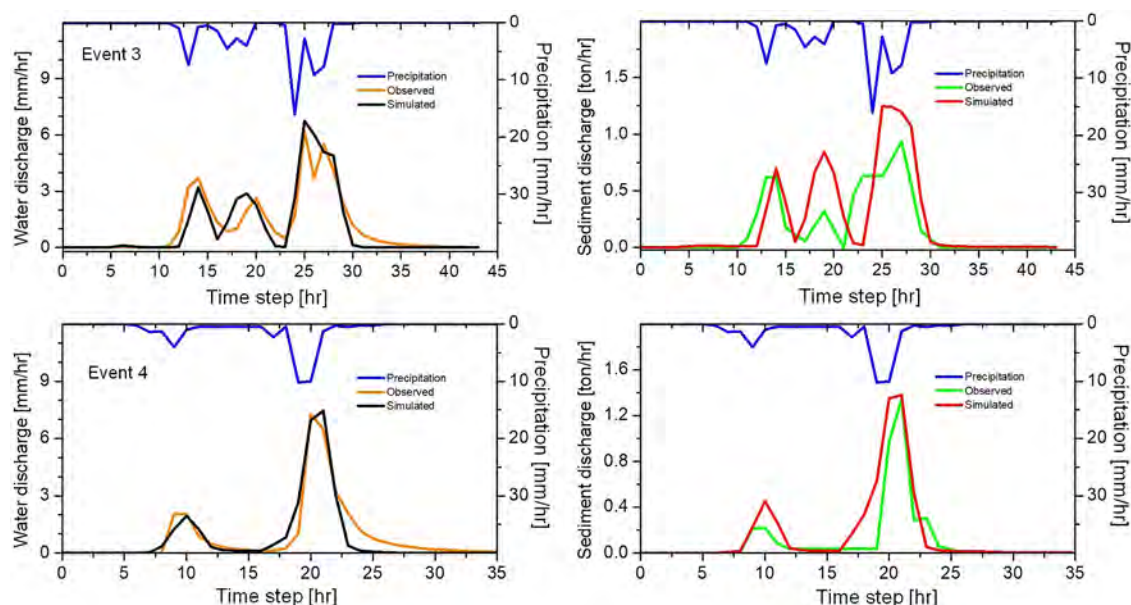
### 3.1.2. Results

Figure 2 presents the hourly rainfall, water discharge, and sediment discharge series for Event 1 and Event 2 during the calibration period of Exp1. All parameters associated with rainfall-runoff and sediment transport processes were manually calibrated, constrained to physically realistic values. The VIC-SED model simulates the hourly water discharge patterns and magnitudes quite well, achieving NSEs greater than 0.7 (Table 2). The

**Table 2**  
Model Performance Statistics of Exp1 for Water Discharge and Sediment Discharge With the Hourly Time Step for the Y2 Watershed

Event	Period	Water discharge			Sediment discharge		
		NSE	RRMSE (%)	Bias (%)	NSE	RRMSE (%)	Bias (%)
Event 1	9:00 a.m., March 8–5:00 a.m., 9 March 2001	0.74	24.03	31.43	0.85	22.85	14.91
Event 2	8:00 a.m., December 15–5:00 a.m., 17 December 2001	0.85	10.64	6.17	0.74	15.54	29.71
Event 3	4:00 a.m., October, 21–23:00 p.m., 22 October 2002	0.82	9.17	6.93	0.59	20.00	−21.77
Event 4	2:00 a.m., December 3–13:00 p.m., 4 December 2002	0.91	10.33	11.73	0.80	22.87	−31.53

Note.  $RRMSE = \sqrt{\frac{1}{d} \sum_{i=1}^d (Q_{s,i} - Q_{o,i})^2} / \bar{Q}_o \times 100\%$ , where  $d$  is the total number of time steps for each event simulation period;  $Q_s$  and  $Q_o$  are the simulated and observed water or sediment discharges;  $\bar{Q}_o$  is the average observed discharge over the event simulation period.



**Figure 3.** Results of Exp1: Hourly water (left) and sediment (right) discharge at the outlet of the USDA-ARS Y2 watershed for events 3 and 4 over the validation period.

sediment discharge is also generally well simulated. However, for event 1, the peak sediment discharge is underestimated at the 8th time step, while the peak water discharge is overestimated at the same time step. In Event 2 at the 32nd–35th time steps, there are significant discrepancies between the simulated and observed sediment discharges, resulting in a total error of up to 29.71% for this event (Table 2). These differences may stem from the model formulation, which does not consider specific soil erosion processes (e.g., the tillage impact) or sediment transport processes. Additionally, the discrepancies could be attributed to errors in sediment observations, as the sediment pattern does not align well with the water discharge process during these time steps.

Figure 3 presents the hourly validation comparison between model simulated water and sediment discharges and the corresponding observations in Event 3 and Event 4 of Exp1. Again, encouraging hourly water discharge comparison results are obtained, and the NSEs are greater than 0.8 for both events. The sediment simulation is also acceptable, especially for Event 4 with NSE of about 0.8. But for Event 3, the simulated sediment shows obvious discrepancies to the observations with NSE less than 0.6 and a relative bias of up to  $-21.77\%$ . In addition to observation uncertainties, these discrepancies are likely caused by the impact of land management activities, such as tillage practice performed on cropland on 26 September 2001, prior to Event 3, which is not considered in the VIC-SED model.

Figure 4 shows comparison results between the observed and simulated suspended sediment at a 15-min time step (water discharges are not shown) from Exp2. The observed sediment time series is obtained by either aggregation (if the actual measurement is less than 15-min) or disaggregation (if the actual measurement is larger than 15-min) in which a linear interpolation between two adjacent measurement data points is used. The breakpoint measurement intervals for the four events are irregular, roughly ranging from 2 to 60 min. For the late portion of Event 3 (i.e., roughly after 90 time steps shown in Figure 4 on 22 October 2002), however, the measurement intervals exceed 120 min, and thus, the observed sediment is actually estimated through disaggregation.

Figure 4 demonstrates that the model successfully reproduced the dynamic variations of sediment discharges during the simulation periods of Events 1, 2, and 4, even using the model parameters calibrated at the hourly time step. The NSEs for these events are approximately 0.6 or higher, with RRMSEs below than 20%, except for Event 4 (see Table 3). For Event 3, similar to the hourly VIC-SED simulation shown in Figure 3, there are again significant discrepancies between simulated and observed sediment discharges. These discrepancies may be attributed to substantial disaggregation errors related to the large measurement intervals (i.e., more than 120-min occurring after 90 time steps in Figure 4) and/or the impact of tillage practices, which are not represented in the VIC-SED model. Additionally, the simple linear interpolation method used may introduce uncertainties in the observed measurements when the interval exceeds 120 min. Thus, the interpolated observed sediment data in

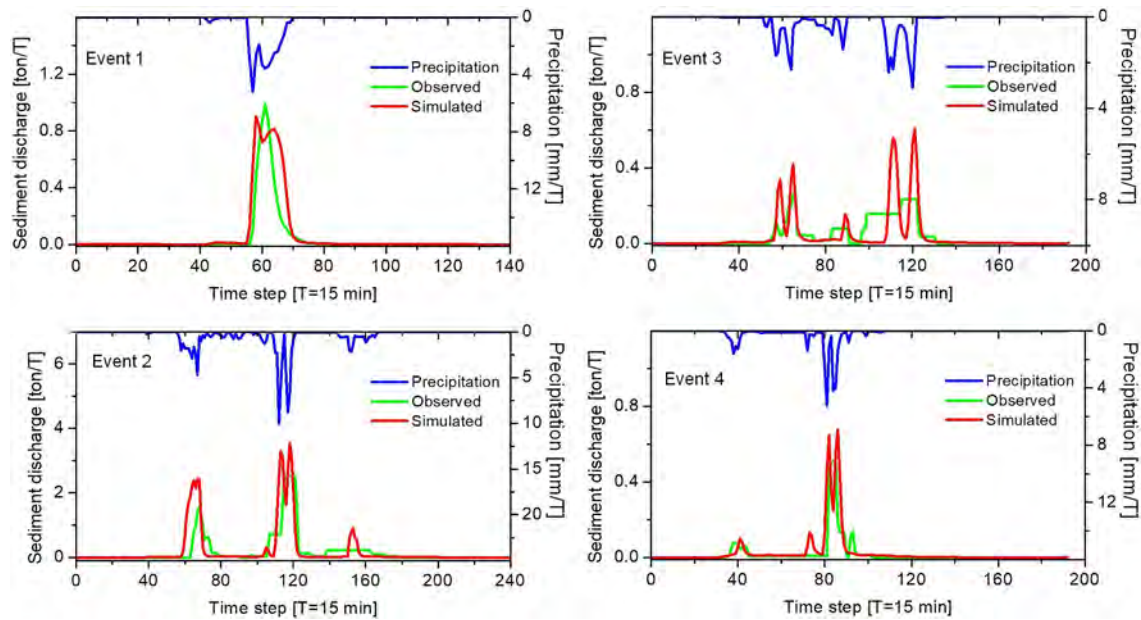


**Figure 4.** Results of Exp2: Comparison of the suspended sediment discharges between the observed and the VIC-SED simulated using 15-min time step over the four storm events at the USDA-ARS Y2 watershed. Water discharges of these four storm events are not shown.

Figure 4 may not adequately reflect the actual behavior of sediment transport during Event 3. This is further evidenced by the inconsistent pattern between the interpolated observed sediment data and the corresponding rainfall variation during Event 3. For example, there is no rainfall between time steps 90 and 110, yet there is a significant amount of interpreted observed sediment during this period (see Event 3 in Figure 4).

Figure 5 compares the daily observed and model simulated sediment discharges for Exp3. The model effectively captures the various levels of sediment discharges, demonstrating an acceptable match with the observations. For 2001, the model achieved an RRMSE of 10.83% and an NSE of 0.76, while for 2002, it achieved an RRMSE of 15.73% and an NSE of 0.67 (see Table 3). However, when the representation of temporal variability of rainfall intensity is removed (i.e., no use of Equation 6) as depicted by Exp4, the model performance declines from Exp3 as expected. The RRMSEs increase from 10.83% to 15.48% for 2001 and from 15.73% to 22.62% for 2002 (see Table 3). Similarly, the NSEs decrease from 0.76 to 0.51 for 2001 and from 0.67 to 0.32 for 2002.

Based on the results of the VIC-SED simulations for Exp1, Exp2, and Exp3, it is evident that VIC-SED performs well in reproducing sediment loads, including their timing and duration, even when a much larger time step (e.g., daily) is used compared to the traditionally used shorter time step (e.g., 15-min). This is despite the model parameters being calibrated at the hourly time step. In fact, the results of Exp2 and Exp3 show that the parameters of VIC-SED are not highly sensitive to the time step used for calibration. However, when the traditional approach of using average precipitation, instead of the distribution, is applied, the simulated sediment discharges deteriorate significantly (see Table 3) across all three measures (i.e., NSE, RRMSE, and Bias) when a large time step (daily) is used.

In addition to these experiments, we conducted another experiment, Exp5, where the VIC-SED model parameters calibrated at daily resolution were then applied to hourly simulations. Compared to the results of Exp1, where the model parameters were calibrated at an hourly resolution, the VIC-SED performance in Exp5 is nearly the same, with only slight degradation (see Figure 6, and Table 4 vs. Table 2). This demonstrates the model's capability to accurately reproduce the magnitudes and dynamics of sediment discharges at finer resolutions, even when calibrated at a coarser resolution.

**Table 3**  
Model Performance Statistics for Suspended Sediment Discharges With the Simulation Time Steps of 15-min (i.e., Exp2) and the Daily (i.e., Exp3 and Exp4), Respectively

Time Step	Events/Periods	NSE	RRMSE (%)	Bias (%)
15 min	Event 1	0.74	19.19	44.69
	Event 2	0.60	13.05	17.09
	Event 3	-0.09	15.51	8.49
	Event 4	0.59	23.03	35.85
Daily	2001	0.76	10.83	-15.54
	2002	0.67	15.73	20.93
	2001 <sup>a</sup>	0.51	15.48	-20.95
	2002 <sup>a</sup>	0.32	22.62	27.24

<sup>a</sup>The representation of temporal variability of rainfall intensity is removed in the simulations.

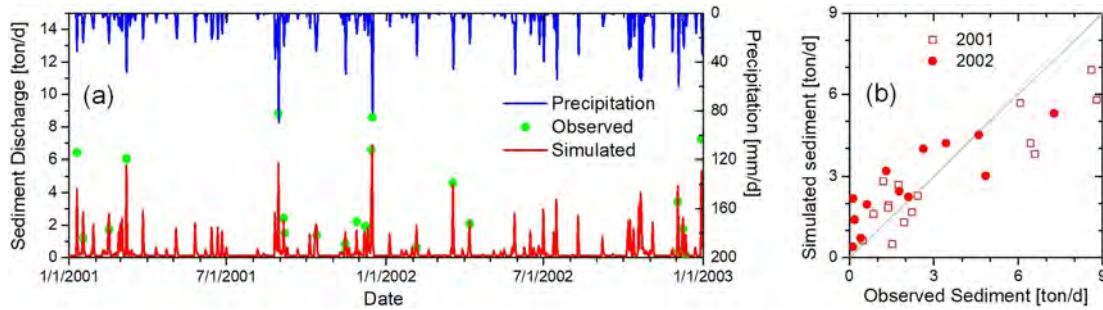


**Figure 5.** Results of Exp3: Comparison of the daily suspended sediment discharges between the observed and the VIC-SED simulated with daily time step at the USDA-ARS Y2 watershed. (a) Time series of sediment discharge (red) and its corresponding rainfall time series (blue) with sediment discharge measurements indicated by green dots, and (b) scatter plot between observed and VIC-SED simulated sediment discharges for the days with measurements available. There are only 15 and 13 days of measurements available in 2001 and 2002, respectively. The calibration period is Year 2001, and validation period is Year 2002.

Results from Exp1, Exp2, Exp3, and Exp5 highlight VIC-SED's effectiveness in mitigating the impact of different temporal resolutions on the model's simulation performance, which is important since the daily data are more widely available than the hourly data. Consequently, users can calibrate the model using daily data and apply those parameters for hourly simulations. Without VIC-SED's approach, calibration would need to occur at each individual resolution to obtain adequate model simulations, as the model parameters are sensitive to the specific resolution used for calibration, as indicated in Exp4.

The encouraging results of Exp2, Exp3, and Exp5 as opposed to Exp4 are expected as they are attributed to the representation of the temporal variability of rainfall intensity using a statistical distribution (i.e., Equation 6) in the formulation of the soil erosion processes within VIC-SED. This is because rainfall intensity is highly variable in time. Using an average over a large time step (e.g., daily) can dramatically mis-represent the temporal rainfall characteristics, and thus lead to large errors. Although using a statistical distribution is also an approximation in representing the reality of rainfall temporal variability, it is a much better approximation than using an average as we know from the statistical theory and other studies where distributions instead of average are used (e.g., Baker et al., 2017; Konapala et al., 2020; H. Li et al., 2011; Liang, Lettenmaier, & Wood, 1996; Liang et al., 2004; Wen et al., 2012). Table 3 clearly illustrates that our new approach of using Equation 6 can significantly relax the

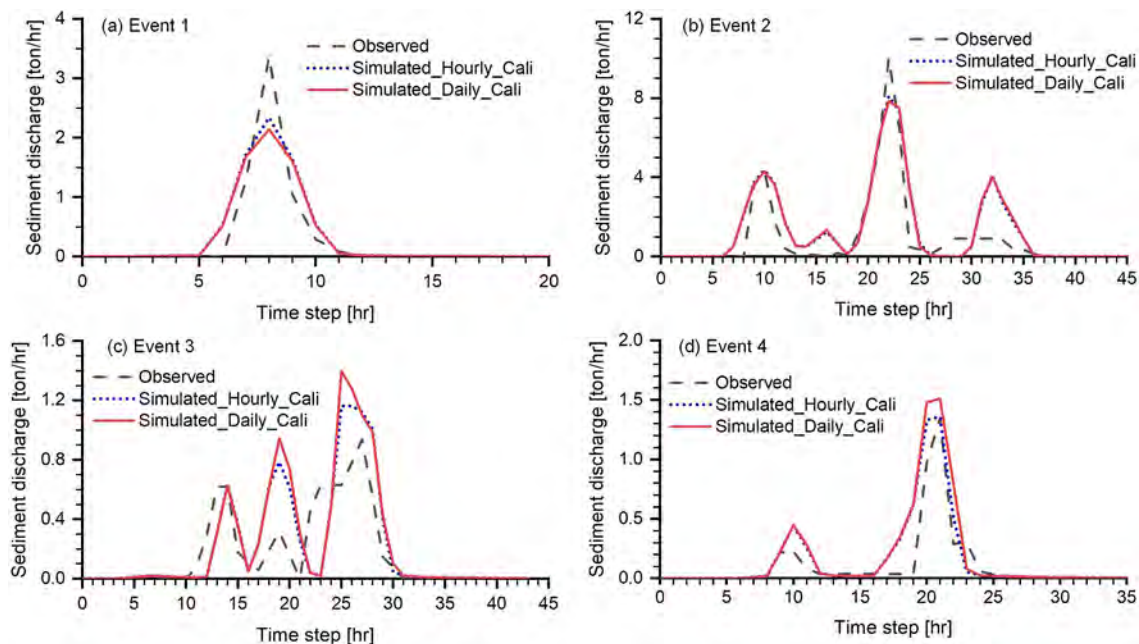


**Figure 6.** Comparison of Exp5 and Exp1 for the four events: The hourly simulation with the parameters calibrated from a daily resolution (Exp5, the red solid line), and the hourly simulation with the parameters calibrated from an hourly resolution (Exp1, the blue dotted line).

**Table 4**  
*Model Performance for Sediment Discharge: Calibrating the Model at a Daily Resolution and Then Applying Those Parameters to an Hourly Simulation*

Time Step	Event/Period	NSE	RRMSE (%)	Bias (%)
Daily	2001–2002	0.78	9.52	6.24
Hourly	Event 1	0.82	24.93	10.11
	Event 2	0.72	15.93	40.10
	Event 3	0.54	22.96	−26.79
	Event 4	0.77	27.95	−38.64

requirements on using high temporal resolution as the required modeling time step and that the model parameters are not sensitive to the time steps used for calibration (see Tables 2–4).

### 3.2. Application of VIC-SED to a Large Watershed With a Coarse Spatial Resolution

In addition to the capability of dealing with a range of temporal resolutions (i.e., from short to large time steps) illustrated in Section 3.1, VIC-SED is also developed with a unique feature of being capable of dealing with a range of spatial scales in representing the sediment and erosion processes which is to be evaluated in this section.

#### 3.2.1. Data Description and Model Setup

The watershed of the Big Darby Creek in Ohio, covering an area of 2,263 km<sup>2</sup>, is shown in Figure 1b. This watershed receives annual mean precipitation of about 900 mm, produces annual mean streamflow of about 250 mm, and generates annual mean sediment discharge up to 41,000 m<sup>3</sup>. The streamflow and sediment generally show a strong seasonal cycle with high discharge during the spring and summer and low discharge during the fall and winter. The predominant land use types are mixed forest (96% of the total area) and the soil is mostly silt loam (92%).

Daily water and suspended sediment discharges were obtained from three gauges operated by United States Geological Survey (USGS). The suspended sediment discharge is computed based on the measured sediment concentration and water discharge. The 1/8th-degree gridded forcing data, that is, the precipitation, temperature and wind speed, at daily time step were produced by Maurer et al. (2002). The same soil property values that are used in the Land Data Assimilation Systems (LDAS) were used in this study for the same 1/8th degree resolution grids. The vegetation information used in the VIC-3L model was extracted from the AVHRR satellites (Hansen et al., 2000). The digital elevation model (DEM) of 90-m grid spacing is used to derive the river network and to compute the fraction of each 1/8th-degree grid that contributes runoff to the connected river segments.

The VIC-SED model is run at a daily time step with the 1/8th-degree spatial resolution. A manual calibration of the VIC-SED model parameters is carried out for the time period of 1/1/1992–12/31/1995 while the default model parameters for soil and vegetation from Maurer et al. (2002) are kept unchanged. The first year is considered as a warm-up period to remove impacts of the initial conditions. The time period of 1/1/1996–9/31/1998 is used to test VIC-SED. This VIC-SED model simulation is called Exp6 in which both the spatial and temporal variability of precipitation is considered.

To investigate impacts of the representation of the spatial-temporal variability of rainfall intensity (i.e., Equations 1 and 6) on sediments, two more model simulations were conducted: (a) not considering both the spatial and the temporal variabilities of the rainfall intensity which is called Exp7, and (b) not considering the spatial variability of rainfall intensity called Exp8. That is, for Exp7 the rainfall intensity is assumed to be evenly distributed across each grid cell of 1/8th degree resolution and within the daily time step as well, while for Exp8, the subgrid variability of rainfall intensity within the 1/8° cell is not considered but the rainfall variability within the daily time step is considered.

#### 3.2.2. Results

Figures 7a and 7b show the simulated water and suspended sediment discharges comparing to their respective observations at the watershed outlet G1 (USGS 03230500) for the calibration period in which both the spatial and temporal subgrid variabilities are considered. As can be observed, the simulated water discharges match the observed series quite well except for a few peak flows. The NSE exceeds 0.7 along with a small relative bias (Table 5). The sediment discharges also generally agree with the observed ones well with its NSE greater than 0.6. Some peak sediment discharges are underestimated and they are consistent with the underestimations of the water discharges. These differences between the model simulations and observations are likely attributable to either the physical processes that are not adequately represented or formulated in the model (e.g., the impact from land management) or the uncertainties of the forcing data or the observations. For example, the simulated water and

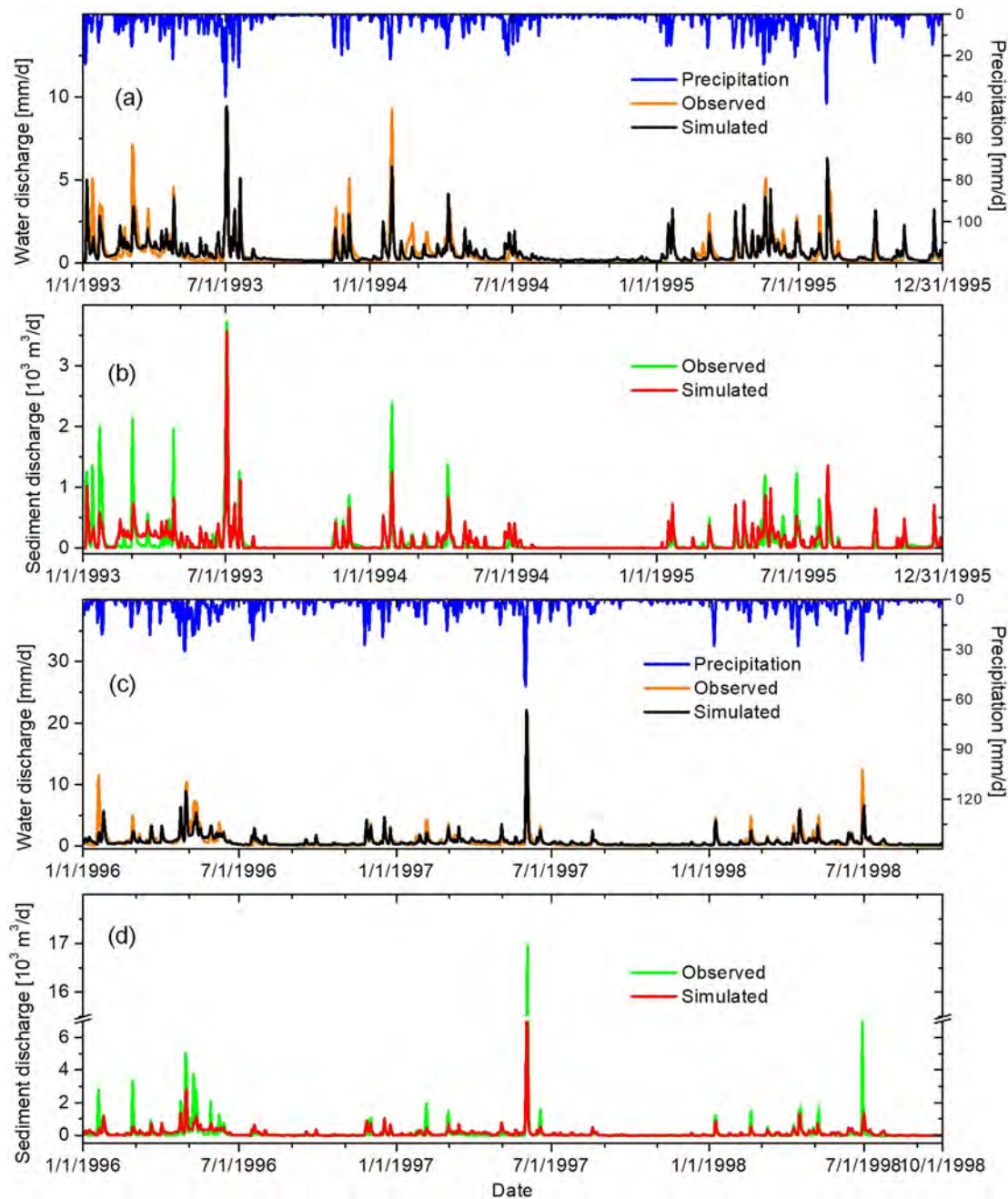


**Figure 7.** Results of Exp6: Comparison of water (a and c) and sediment (b and d) discharges between the observations and the VIC-SED model simulations at the gauge G1 (USGS 03230500) for the calibration (a and b) and validation (c and d) periods.

sediment discharges on January 13 and March 5 in 1993 correspond to small rainfall events, but the observed water and sediment discharges are quite high.

Figures 7c and 7d show results over the testing (validation) period. It can be observed that the new model, VIC-SED, can reproduce both the water and sediment discharge series well and the biases are about 2.75% and  $-5.30\%$  (Table 5), for water and sediment, respectively. On the other hand, a few peak sediment discharges are significantly underestimated as shown in Figure 7d resulting in a low NSE value of 0.45. For instance, there are relatively large discrepancies in magnitude between the simulated and observed sediments on 19 January 1996 and 29 June 1998, but their timing and durations are reasonably simulated. The true reasons causing these

**Table 5**  
Model Performance Statistics for Water Discharge and Sediment Discharge of Exp6 in the Big Darby Creek Watershed

Period	Gauge	Water discharge			Sediment discharge		
		NSE	RRMSE (%)	Bias (%)	NSE	RRMSE (%)	Bias (%)
Calibration (1/1/1993–12/31/1995)	G1 (03230500)	0.71	2.70	3.87	0.63	12.22	20.45
Validation (1/1/1993–12/31/1995)	G2 (03230450)	0.63	3.29	10.21	0.57	7.09	32.28
	G3 (03230310)	0.59	29.78	15.72	0.61	12.71	18.30
Validation (1/1/1996–9/31/1998)	G1 (03230500)	0.65	3.64	2.75	0.45	11.98	−5.30
	G2 (03230450)	0.62	14.98	−5.23	0.58	6.26	38.79
	G3 (03230310)	0.65	11.20	−10.21	0.80	6.35	21.31

underestimations by VIC-SED could be complex due to multiple factors involved. More data and information are needed to have a concrete analysis on them.

In addition to the encouraging model simulations at the watershed outlet G1, VIC-SED also performs well in simulating flow and sediment load at the two inner gauges of G2 (03230450) and G3 (03230310) in which the model parameters calibrated with data from G1 are applied. In other words, the observed data from 1/1/1993 to 12/31/1995 for the two inner outlets corresponding to the gauges of G2 and G3 are not used to calibrate the VIC-SED model parameters, that is, the VIC-SED model parameters used for the subwatersheds with outlets of G2 and G3, respectively, are the same as those used for the entire watershed with the outlet at G1.

Figure 8 shows the comparisons between VIC-SED simulated and observed sediment discharges over the 2nd validation period of 1/1/1996 to 9/31/1998 at each of the two inner gauges. Table 5 shows that the NSEs and RRMSEs at G2 and G3 are generally similar to those at the outlet G1 except for the Bias metrics which are relatively larger (especially for the subwatershed with the G2 outlet) for both the water discharge and the sediment discharges for the two validation periods. The larger discrepancy for G2 than for G3 is expected as G2 corresponds to the smallest drainage area of 86 km<sup>2</sup> which is much smaller than the 1/8° modeling resolution. However, due to VIC-SED's use of rainfall distribution (i.e., Equation 1) to account for impacts of the rainfall spatial subgrid variability on the rainfall kinetic energy (see Equations 7 and 8), the impact of the rainfall intensity due to a coarser spatial resolution (i.e., 1/8°) is limited as shown by the metrics in Table 5 which is also expected.

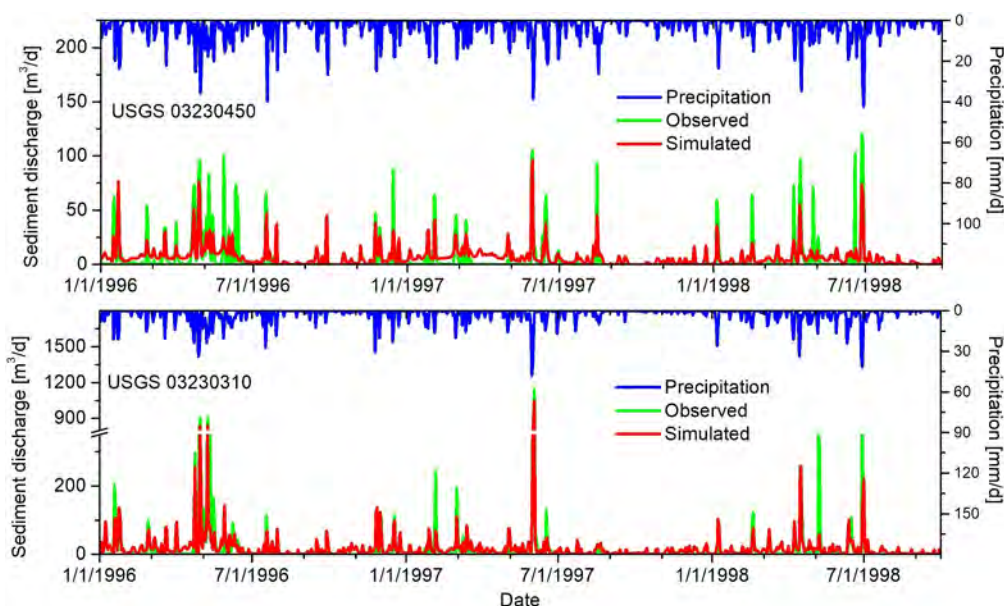


**Figure 8.** Results of Exp6: Comparison of sediment discharges between the observations and the VIC-SED simulations at the inner gauge G2 (upper panel) and gauge G3 (lower panel) for the 2nd validation period.

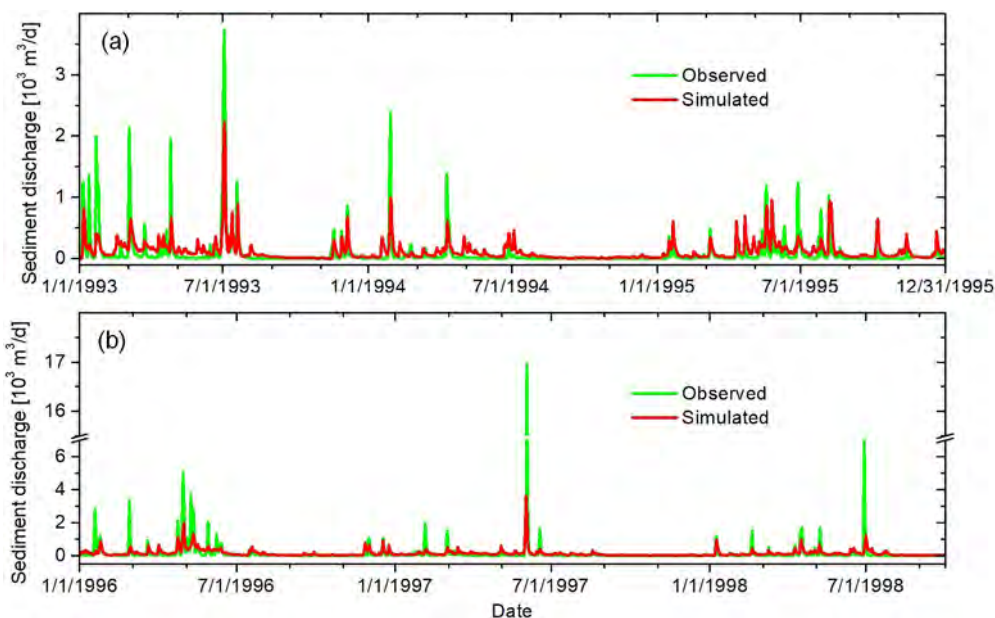


**Figure 9.** Results of Exp7: Suspended sediment discharges of gauge G1 (USGS 03230500) when both of the spatial and the temporal variabilities of rainfall intensity are not considered: (a) Calibration and (b) Validation.

In summary, these validation results for the period of 1/1/1996–9/31/1998 at G1 and for the entire period between 1/1/1993 and 9/31/1998 at G2 and G3 are quite encouraging as no calibrations were carried out at these two inner gauges. These results (Figures 7 and 8, and Table 5) collectively illustrate the relative robustness of VIC-SED to the use of large spatial resolution of rainfall and model parameters.

Figure 9a shows the VIC-SED model simulated results at the outlet G1 for its calibration period when both the spatial and temporal variabilities in the rainfall intensity are not considered (i.e., Exp7). The model significantly underestimates the peak sediment discharge of 3 July 1993 and a few other sediment peak discharges as compared to the result of the same day (see Figure 7b) when both the spatial and temporal variabilities of rainfall intensity are considered. Such underestimations are expected because the use of average rainfall intensity with a coarse modeling resolution (both in space and time) would significantly reduce the rainfall intensity, and thus reduce the rainfall kinetic energy. These impacts are significant even when the VIC-SED model parameters are calibrated for the period shown in Figure 9a to partially compensate the reduced rainfall intensity for the period. Similar underestimations of the peak sediment discharges are also observed in Figure 9b over the validation period compared to Figure 7d. For example, the peak sediment discharge around 1 June 1997 shown in Figure 9b is only about half of the amount shown in Figure 7d and about 1/3 of the observations for the same time. Degradation of the model's performance on the sediment discharge simulations at the two inner outlets is also present. Table 6 shows the statistics of the sediment discharge simulations for all three gauges. The NSEs and RRMSE are significantly improved by considering both the spatial and temporal variabilities of the rainfall (i.e., Exp6) with the VIC-SED model presented in this work. Considering only the temporal variability of rainfall but not its subgrid spatial variability improves the model performance in terms of NSEs to some extent, while the improvements on the relative bias measure are mixed. Overall, the performance on simulating the sediment discharge is much better when both the spatial and temporal variabilities of the rainfall in VIC-SED are accounted for.

Our results demonstrate that it is fundamentally important to have the spatio-temporal variability of rainfall intensity represented if the model application is to a large modeling grid cell (e.g., 1/8th degree) and at a daily time step. Without considering the spatial and temporal variabilities of the rainfall intensity, the model cannot reproduce the general pattern of the sediment discharge. This study illustrates the feasibility of VIC-SED for conducting coarse-resolution modeling for large scale soil erosion and sediment studies when such rainfall variabilities are accounted for.

**Table 6**  
Model Performance Statistics for Suspended Sediment Discharge When Spatio-Temporal Variability of Rainfall Intensity (Exp7) or the Spatial Variability of Rainfall (Exp8) Is Not Considered

Period	Gauge	No Spatial- Var. <sup>a</sup>			No Spatial and Temporal Var. <sup>b</sup>		
		NSE	RRMSE (%)	Bias (%)	NSE	RRMSE (%)	Bias (%)
Calibration (1/1/1993–12/31/1995)	G1 (03230500)	0.54	11.17	41.64	0.50	12.10	44.83
	G2 (03230450)	0.38	10.99	52.77	0.25	16.10	49.85
	G3 (03230310)	0.45	12.08	41.85	0.42	12.97	41.98
Validation (1/1/1996–9/31/1998)	G1 (03230500)	0.29	13.59	−8.57	0.26	13.95	−10.39
	G2 (03230450)	0.40	9.21	48.92	0.17	19.41	40.83
	G3 (03230310)	0.51	9.86	22.76	0.36	12.75	28.87

<sup>a</sup>No Spatial Var. represents the case without considering the spatial variability of rainfall intensity within the 1/8° resolution but accounting for its temporal variability within the daily time step (i.e., Exp8). <sup>b</sup>No Spatial and Temporal Var. represents the case without considering the spatio-temporal variability of rainfall intensity (i.e., Exp7).

#### 4. Parameter Sensitivity Analysis

Studies have shown that the VIC-3L and MSR models are insensitive to their model parameters compared to other similar types of models (e.g., Baker et al., 2017; Konapala et al., 2020; H. Li et al., 2011; Liang, Wood, & Lettenmaier, 1996; Liang & Guo, 2003; Liang et al., 2004; Prentice et al., 2015; Wen et al., 2012) due to their explicit representation of the subgrid-scale variability of soil, vegetation, and flow path length in VIC-3L and MSR. Therefore, we will focus on investigating the sensitivity of the four newly introduced parameters (Table 1) related to the SED process in VIC-SED in this section. To examine their sensitivities, we conducted several simulations in which their values were changed over a wide range of up to 50% with respect to their calibrated values. The final range of each parameter is constrained by its lower and upper bounds.

For the watershed Y2 of USDA-ARS, the model was run at an hourly time step with different parameter values, changing one parameter at a time. Figure 10 shows the sensitivity results for Event 2. Parameters  $k_r$  (Equation 5) and  $\alpha$  (Equation 10) demonstrate limited impacts on the simulated suspended sediment discharges. Since watershed Y2 is very small (about 0.534 km<sup>2</sup>), it is likely that the spatial variability of rainfall intensity is small, leading to the simulated sediment insensitive to the parameter  $k_r$ . However, the sediment discharges are sensitive

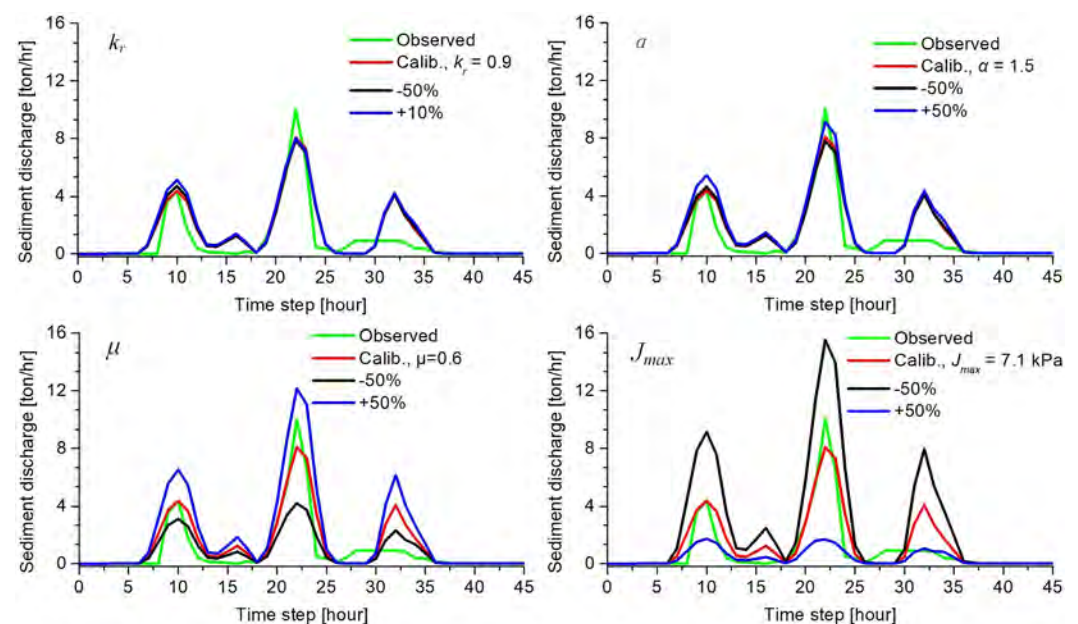


**Figure 10.** Parameter sensitivity results at the USDA-ARS Y2 watershed for Event 2.

**Table 7**  
Parameter Sensitivity for the USDA-ARS Y2 Watershed for Event 2<sup>a</sup>

Errors	$k_r$		$\alpha$		$\mu$		$J_{\max}$	
	+10%	-50%	+50%	-50%	+50%	-50%	+50%	-50%
NSE	0.73	0.68	0.74	0.65	0.67	0.16	-1.06	0.32
RRMSE (%)	16.07	17.40	15.92	18.29	17.88	28.42	44.46	25.59
Bias (%)	42.68	51.65	41.20	57.21	9.86	108.68	177.40	-55.52

<sup>a</sup>In Section 3.1.2, the values of calibrated parameters are:  $k_r = 0.9$ ,  $\alpha = 1.5$ ,  $\mu = 0.6$ , and  $J_{\max} = 7.1$  kPa, and the performance statistics are shown in Table 2.

to parameters  $\mu$  and  $J_{\max}$  (Equation 13). An increase of 50% in  $J_{\max}$  would result in a relative change of simulated sediment discharge to be over 177% (Table 7) compared to the sediment discharge with the calibrated value for  $J_{\max}$ . The large sensitivities of parameters  $\mu$  and  $J_{\max}$  are probably due to the expressions of Equations 11 and 12 where the net detachment of soil particles by flow ( $DF$ ) varies exponentially with  $J$  which is a function of  $\mu$  and  $J_{\max}$ . It is worth mentioning that the two sensitive parameters,  $\mu$  and  $J_{\max}$ , are not the new parameters introduced by our new approach related to the consideration of the spatial and temporal distribution of the rainfall intensity,  $k_r$ , nor the new parameter  $\alpha$  introduced in Equation 10; rather they are the existing parameters related to Equations 11–13, which are widely accepted and used in the community.

To further investigate the sensitivity of the newly introduced parameter,  $k_r$ , we did the sensitivity analysis for the large watershed in Ohio where  $k_r$  was investigated over a period with large rainfall in which notable soil erosion occurred. The calibrated value of  $k_r$  is 0.5 for this watershed. Figure 11 shows the simulated sediment discharge for different values of  $k_r$ , from June 20 to 20 July 1993. The sediment discharge is underestimated by 18.5% (overestimated by 45.6%) due to the decrease (increase) of the parameter  $k_r$  by 50%. This indicates that the sediment discharge at this large watershed is more sensitive to the parameter  $k_r$  (Equation 5) than that at the small watershed, but comparing its sensitivity to parameters,  $\mu$  and  $J_{\max}$ ,  $k_r$  is much less sensitive. In applications of the VIC-SED model, it is better to first calibrate the most sensitive parameters  $\mu$  and  $J_{\max}$ , then  $kr$ , and then the other ones.

Please note the method of changing one parameter at a time is a simple parameter sensitivity analysis approach. There are numerous of other sensitivity analysis methods which can be used to provide more comprehensive evaluations, such as the randomized one-factor-at-a-time method (Morris, 1991), the combination of latin-hypercube and one-factor-at-a-time sampling method (van Griensven et al., 2006), and the Monte Carlo framework (Demaria et al., 2007).

## 5. Conclusions and Future Work

Although numerous soil erosion and sediment transport models exist, they are primarily developed based on theories and experiments applicable at a hillslope or small scales. These models typically focus on total soil loss over a storm period rather than the dynamic sediment discharge within a storm. Additionally, they often require high-resolution data and expensive computational resources, limiting their applications for long-term dynamics of erosion and sediment yields, especially at regional and global scales.

In this study we present a new continuous model, VIC-SED, designed for large watersheds or large-scale studies with coarse spatial (e.g., 10 km) and temporal (e.g., daily time step) resolutions over long periods. The VIC-SED model addresses challenges related to the subgrid and subtime variabilities of rainfall on soil erosion processes. To reduce biases in soil detachment by rainfall at coarse resolutions, the spatial variability of rainfall intensity is statistically represented with a lognormal distribution (Equation 1), and the temporal variability is characterized with an exponential distribution (Equation 6). VIC-SED uses process-based equations to describe soil detachment and transport processes, and employs empirically based equations for other

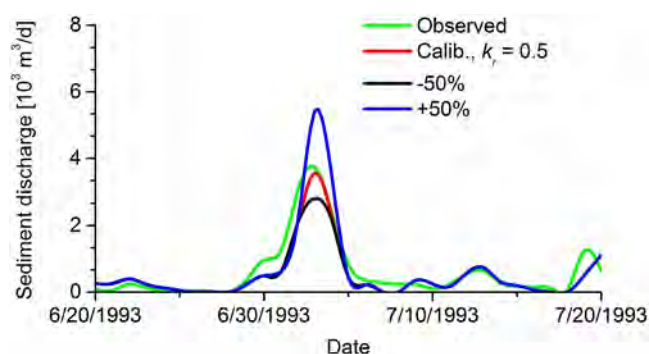


**Figure 11.** The sensitivity of parameter  $k_r$  for the Ohio watershed at gauge G1 (USGS 03230500) over a period of June 20–20 July 1993.

processes relevant to erosion and sediment, similar to other widely used sediment models. The empirically based equations help compensate for physical processes that are not yet well formulated or understood. Additionally, impacts of subgrid spatial variability of soil heterogeneity and vegetation, and of overland flow path length on various hydrological processes are considered through the large-scale VIC-3L land surface model in conjunction with a multi-scale routing (MSR) framework. Therefore, the consideration of subgrid spatial variability makes VIC-SED unique and suitable for investigating large-scale soil erosion and sediment dynamics using coarse spatial and temporal resolutions.

The VIC-SED model has been successfully applied to simulate water and sediment discharges in both a small watershed (USDA-ARS Y2) and a large watershed (Big Darby Creek watershed) with promising results. In the small watershed, VIC-SED effectively reproduced soil erosion and sediment transport processes using both short (e.g., 15 min) and long (e.g., daily) time steps. However, when the temporal variability of rainfall intensity in VIC-SED is turned off, the model performance at the daily time step degrades, highlighting the importance of subgrid variability of rainfall intensity on erosion processes. In the large watershed, with a coarse modeling spatial resolution of 1/8th degree, VIC-SED also performed well, as illustrated by comparisons between model-simulated and observed suspended sediment discharges from three gauges within the watershed. The results indicate that when spatio-temporal variability of rainfall intensity is considered, the VIC-SED simulated sediment discharges closely match observations; when this variability is not considered, the VIC-SED simulated sediment discharges deteriorate significantly. The model introduces four new parameters, with those related to soil cohesion (i.e.,  $\mu$  and  $J_{\max}$ ) being the most sensitive. Parameter sensitivity may vary by watershed, so it is recommended to calibrate the most sensitive parameters first.

The preliminary results highlight VIC-SED's strengths and the significance of considering subgrid spatio-temporal variability of rainfall in erosion processes. While the initial simulations are promising, further evaluations are needed, such as applying VIC-SED to watersheds with more complex stream networks and testing it at regional and global scales using global sediment data sets (Tan et al., 2017, 2018), where the modeling cell size is on the order of 1/8th degree or larger. Future improvements could include incorporating processes like stream bank erosion, bed load transport, and floodplain storages, which are important for large-scale SED applications. Additionally, the impact of land management on soil erosion should be included in future developments.

Since VIC-SED is developed based on several other sediment models (e.g., EUROSEM, SWAT), we plan to investigate its strengths and limitations compared to these models at large scales. VIC-SED can serve as a promising baseline for studies on soil erosion risk, lateral carbon transfer, environmental zoning and vulnerability in large watershed and regional scales. It has the potential to identify sensitivity of suspended sediment yields to the changes in climate, land cover, and land use.

## Appendix A: Point-Scale Rainfall Energy

Rainfall kinetic energy is well formulated in Brandt (1989, 1990) and related equations have been included in the EUROSEM model (Morgan et al., 1998). The point-scale direct throughfall energy is expressed as:

$$KE_{DT,point} = 8.95 + 3.67 \cdot \ln r_{i,t}, \quad (A1)$$

where  $KE_{DT,point}$  is rainfall energy of direct throughfall ( $WL^2/L$ ),  $r_{i,t}$  ( $r_{i,t} > 0$ ) is the rainfall intensity (L/T) at location  $i$  and time  $t$ . The energy of leaf drip is estimated with the relationship of plant height (Brandt, 1990):

$$KE_{LD} = (15.8 \cdot PH^{0.5}) - 5.87, \quad (A2)$$

where  $PH$  is the effective height of the plant canopy (L) which is defined in VIC-3L as a vegetation parameter (see Table 1). If  $PH < 0.14$  m,  $KE_{LD} = 0$ . So, the total kinetic energy  $KE$  ( $WL^2$ ) of the rainfall during a time step:

$$KE_{point} = KE_{DT,point} \cdot (1 - f_c) \cdot R_{Total} + KE_{LD} \cdot f_c \cdot R_{Net}, \quad (A3)$$

where  $R_{\text{Total}}$  (mm) and  $R_{\text{Net}}$  (mm) are the total rainfall and the net rainfall, respectively, for the time step;  $R_{\text{Net}}$  is the residual of  $R_{\text{Total}}$  minus the maximum canopy interception; and  $f_c$  is the fraction of canopy cover which is estimated by the leaf area index (Nilson, 1971) as follows,

$$f_c = 1 - \exp(-0.5 \cdot \text{LAI}), \quad (\text{A4})$$

where LAI is the leaf area index and it can be derived from remote sensing retrievals.

### Appendix B: Adjustment Factor of Water Ponding Effect

The water ponding effect on soil detachment has a strong relationship with generated runoff, and it is well formulated in Kabir et al. (2011):

$$F_h = \begin{cases} \exp(1 - h/D_m), & h > D_m \\ 1, & h \leq D_m \end{cases}, \quad (\text{B1})$$

$$D_m = 0.00124 \cdot \bar{r}^{0.182}, \quad (\text{B2})$$

where  $F_h$  is the adjustment factor accounting for water ponding.  $h$  is the mean depth of the surface water (i.e., surface runoff depth) (L) and it can be computed from a hydrological model (e.g., VIC-3L).  $D_m$  is the median raindrop diameter (L),  $\bar{r}$  is the spatio-temporal averaged rainfall intensity (L/T), that is, the rainfall intensity averaged over a modeling grid cell in space and duration  $\Delta t$  in time. The equation for water ponding effect may be superior to the one used in EUROSEM (Morgan et al., 1998), since it does not introduce any parameters and it accounts for the impacts of raindrop diameter size (Kabir et al., 2011).

### Appendix C: Settling Velocity and Transport Capacity Concentration

The settling velocity  $\omega_s$  (L/T) in Equation 11 is estimated with the equation proposed by (Dietrich, 1982; Ferguson & Church, 2004):

$$\omega_s = \frac{S_p \cdot g \cdot d_{50}^2}{C_1 \cdot \nu + (0.75 \cdot C_2 \cdot S_p \cdot g \cdot d_{50}^3)}, \quad (\text{C1})$$

where  $S_p$  is the submerged specific gravity (1.65 for quartz in water),  $g$  is the acceleration due to gravity (L/T<sup>2</sup>),  $\nu$  is the kinematic viscosity of the water (10<sup>-6</sup> kg/m/s at 20°C), and  $d_{50}$  is the median particle size of the soil (L).  $C_1$  and  $C_2$  are two parameters with suggested values of 18 and 1.0, respectively, for intermediate grains of varied shape (Ferguson & Church, 2004).

The transport capacity concentration  $TC$  (L<sup>3</sup>/L<sup>3</sup>) is based on a unit stream power ( $\omega$ ), following the work of Govers (1990) which is used in Morgan et al. (1998):

$$TC = c \cdot (\omega - \omega_{cr})^\eta, \quad (\text{C2})$$

$$\omega = 10 \cdot U \cdot S, \quad (\text{C3})$$

$$c = [(d_{50} + 5)/0.32]^{-0.6}, \quad (\text{C4})$$

$$\eta = [(d_{50} + 5)/300]^{0.25}, \quad (\text{C5})$$

where  $\omega$  is the unit stream power (L/T),  $\omega_{cr}$  is the critical value of unit stream power (0.4 cm/s) (Govers, 1990),  $U$  is the mean flow velocity (L/T),  $S$  is the slope (%) and is assumed uniform within a computational grid,  $c$  and  $\eta$  are coefficients experimentally derived from particle size (Miller et al., 2012; Morgan et al., 1998).

## Data Availability Statement

Open Research Associated the program code of VIC-SED, the forcing and parameters, and the observed and simulated water and sediment discharge for the two watersheds in this study are available via the repository (Xie & Liang, 2024).

## Acknowledgments

We would like to acknowledge Dr. Zhiqun Wen for his help in using the multi-scale runoff routing computer code. We also thank the anonymous reviewers for constructive comments and suggestions. This work was partially supported by a grant from the National Natural Science Foundation of China (42271021) to the first author. Co-author, Xu Liang, acknowledges the partial support from the William Kepler Whiteford Professorship from the University of Pittsburgh.

## References

- Abaci, O., & Papanicolaou, A. (2009). Long-term effects of management practices on water-driven soil erosion in an intense agricultural sub-watershed: Monitoring and modelling. *Hydrological Processes*, 23(19), 2818–2837. <https://doi.org/10.1002/hyp.7380>
- Aksoy, H., & Kavvas, M. L. (2005). A review of hillslope and watershed scale erosion and sediment transport models. *Catena*, 64(2–3), 247–271. <https://doi.org/10.1016/j.catena.2005.08.008>
- Allen, P. M., Arnold, J. G., & Jakubowski, E. (1999). Prediction of stream channel erosion potential. *Environmental and Engineering Geoscience*, 5(3), 339–351. <https://doi.org/10.2113/gsegeosci.v.3.339>
- Allen, P. M., Harmel, R., Arnold, J. G., Plant, B., Yelderman, J., & King, K. (2005). Field data and flow system response in clay (vertisol) shale terrain, north central Texas, USA. *Hydrological Processes*, 19(14), 2719–2736. <https://doi.org/10.1002/hyp.5782>
- Arnold, J. G., Allen, P. M., & Bernhardt, G. (1993). A comprehensive surface-groundwater flow model. *Journal of Hydrology*, 142(1–4), 47–69. [https://doi.org/10.1016/0022-1694\(93\)90004-s](https://doi.org/10.1016/0022-1694(93)90004-s)
- Arnold, J. G., Moriasi, D., Gassman, P., Abbaspour, K., White, M., Srinivasan, R., et al. (2012). SWAT: Model use, calibration, and validation. *Transactions of the American Society of Agricultural and Biological Engineers*, 55(4), 1491–1508. <https://doi.org/10.13031/2013.42256>
- Arnold, J. G., Srinivasan, R., Mutiah, R. S., & Allen, P. M. (1999). Continental scale simulation of the hydrologic balance. *JAWRA Journal of the American Water Resources Association*, 35(5), 1037–1051. <https://doi.org/10.1111/j.1752-1688.1999.tb04192.x>
- Baets, S. D., Torri, D., Poesen, J., Salvador, M. P., & Meersmans, J. (2008). Modelling increased soil cohesion due to roots with EUROSEM. *Earth Surface Processes and Landforms*, 33(13), 1948–1963. <https://doi.org/10.1002/esp.1647>
- Baker, I. T., Sellers, P. J., Denning, A. S., Medina, I., Kraus, P., Haynes, K. D., & Biraud, S. C. (2017). Closing the scale gap between land surface parameterizations and GCMs with a new scheme, SiB3-Bins. *Journal of Advances in Modeling Earth Systems*, 9(1), 691–711. <https://doi.org/10.1002/2016ms000764>
- Brandt, C. J. (1989). The size distribution of throughfall drops under vegetation canopies. *Catena*, 16(4), 507–524. [https://doi.org/10.1016/0341-8162\(89\)90032-5](https://doi.org/10.1016/0341-8162(89)90032-5)
- Brandt, C. J. (1990). Simulation of the size distribution and erosivity of raindrops and throughfall drops. *Earth Surface Processes and Landforms*, 15(8), 687–698. <https://doi.org/10.1002/esp.3290150803>
- Bryan, R. B. (2000). Soil erodibility and processes of water erosion on hillslope. *Geomorphology*, 32(3–4), 385–415. [https://doi.org/10.1016/S0169-555X\(99\)00105-1](https://doi.org/10.1016/S0169-555X(99)00105-1)
- Cherkauer, K. A., & Lettenmaier, D. P. (1999). Hydrologic effects of frozen soils in the upper Mississippi River basin. *Journal of Geophysical Research*, 104(D16), 19599–19610. <https://doi.org/10.1029/1999jd900337>
- Cho, H. K., Bowman, K. P., & North, G. R. (2004). A comparison of gamma and lognormal distributions for characterizing satellite rain rates from the Tropical Rainfall Measuring Mission. *Journal of Applied Meteorology*, 43(11), 1586–1597. <https://doi.org/10.1175/jam2165.1>
- Demaria, E. M., Nijssen, B., & Wagener, T. (2007). Monte Carlo sensitivity analysis of land surface parameters using the Variable Infiltration Capacity model. *Journal of Geophysical Research*, 112(D11), D11113. <https://doi.org/10.1029/2006jd007534>
- de Vente, J., & Poesen, J. (2005). Predicting soil erosion and sediment yield at the basin scale: Scale issues and semi-quantitative models. *Earth-Science Reviews*, 71(1–2), 95–125. <https://doi.org/10.1016/j.earscirev.2005.02.002>
- Dietrich, W. E. (1982). Settling velocity of natural particles. *Water Resources Research*, 18(6), 1615–1626. <https://doi.org/10.1029/WR018i006p01615>
- Ferguson, R. I., & Church, M. (2004). A simple universal equation for grain settling velocity. *Journal of Sedimentary Research*, 74(6), 933–937. <https://doi.org/10.1306/051204740933>
- Flanagan, D. C., Frankenberger, J., Cochrane, T., Renschler, C., & Elliot, W. (2013). Geospatial application of the water erosion prediction project (WEPP) model. *Transactions of the American Society of Agricultural and Biological Engineers*, 56(2), 591–601. <https://doi.org/10.13031/2013.42681>
- Flanagan, D. C., & Nearing, M. A. (1995). USDA-water erosion prediction project: Hillslope profile and watershed model documentation. NSERL report, 10, 1196–47097.
- Fredlund, D. G., Xing, A., Fredlund, M. D., & Barbour, S. (1995). The relationship of the unsaturated soil shear strength function to the soil water characteristic curve. *Canadian Geotechnical Journal*, 32, 440–448. <https://doi.org/10.1139/96-065>
- Govers, G. (1990). *Empirical relationships for the transport capacity of overland flow* (Vol. 189, pp. 45–63). IAHS publication.
- Guo, J., Liang, X., & Leung, L. R. (2004). A new multiscale flow network generation scheme for land surface models. *Geophysical Research Letters*, 31(23), L233502. <https://doi.org/10.1029/2004gl021381>
- Hansen, M. C., Defries, R. S., Townshend, J. R. G., & Sohlberg, R. (2000). Global land cover classification at 1 km spatial resolution using a classification tree approach. *International Journal of Remote Sensing*, 21(6–7), 1331–1364. <https://doi.org/10.1080/014311600210209>
- Huang, M., & Liang, X. (2006). On the assessment of the impact of reducing parameters and identification of parameter uncertainties for a hydrologic model with applications to ungauged basins. *Journal of Hydrology*, 320(1), 37–61. <https://doi.org/10.1016/j.jhydrol.2005.07.010>
- Istanbulluoglu, E., & Bras, R. L. (2006). On the dynamics of soil moisture, vegetation, and erosion: Implications of climate variability and change. *Water Resources Research*, 42(6), W06418. <https://doi.org/10.1029/2005wr004113>
- Jain, M. K., Kothiyari, U. C., & Raju, K. G. (2005). GIS based distributed model for soil erosion and rate of sediment outflow from catchments. *Journal of Hydraulic Engineering*, 131(9), 755–769. [https://doi.org/10.1061/\(asce\)0733-9429\(2005\)131:9\(755\)](https://doi.org/10.1061/(asce)0733-9429(2005)131:9(755))
- Jeong, J., Kannan, N., Arnold, J. G., Glick, R., Gosselink, L., Srinivasan, R., & Harmel, R. (2011). Development of sub-daily erosion and sediment transport algorithms for SWAT. *Transactions of the Asabe*, 54(5), 1685–1691. <https://doi.org/10.13031/2013.39841>
- Kabir, M., Dutta, D., & Hironaka, S. (2011). Process-based distributed modeling approach for analysis of sediment dynamics in a river basin. *Hydrology and Earth System Sciences*, 15(4), 1307–1321. <https://doi.org/10.5194/hess-15-1307-2011>
- Konapala, G., Kao, S. C. E., & Addor, N. (2020). Exploring hydrologic model process connectivity at the continental scale through an information theory approach. *Water Resources Research*, 56(10), e2020WR027340. <https://doi.org/10.1029/2020wr027340>

- Kundu, P. K., & Siddani, R. K. (2007). A new class of probability distributions for describing the spatial statistics of area-averaged rainfall. *Journal of Geophysical Research*, *112*(D18), D18113. <https://doi.org/10.1029/2006jd008042>
- Lafren, J., Elliot, W., Simanton, J., Holzhey, C., & Kohl, K. (1991). WEPP: Soil erodibility experiments for rangeland and cropland soils. *Journal of Soil and Water Conservation*, *46*(1), 39–44.
- Latocha, A., Szymanowski, M., Jeziorska, J., Stec, M., & Roszczewska, M. (2016). Effects of land abandonment and climate change on soil erosion—An example from depopulated agricultural lands in the Sudetes Mts., SW Poland. *Catena*, *145*, 128–141. <https://doi.org/10.1016/j.catena.2016.05.027>
- Leung, L. R., Huang, M., Qian, Y., & Liang, X. (2010). Climate-soil-vegetation control on groundwater table dynamics and its feedbacks in a climate model. *Climate Dynamics*, *36*(1–2), 1–25. <https://doi.org/10.1007/s00382-010-0746-x>
- Li, H., Huang, M., Wigmosta, M. S., Ke, Y., Coleman, A. M., Leung, L. R., et al. (2011). Evaluating runoff simulations from the Community Land Model 4.0 using observations from flux towers and a mountainous watershed. *Journal of Geophysical Research*, *116*(D24), D24120. <https://doi.org/10.1029/2011jd016276>
- Li, P. F., Mu, X. M., Holden, J., Wu, Y. P., Irvine, B., Wang, F., et al. (2017). Comparison of soil erosion models used to study the Chinese Loess Plateau. *Earth-Science Reviews*, *170*, 17–30. <https://doi.org/10.1016/j.earscirev.2017.05.005>
- Liang, X., & Guo, J. Z. (2003). Intercomparison of land-surface parameterization schemes: Sensitivity of surface energy and water fluxes to model parameters. *Journal of Hydrology*, *279*(1–4), 182–209. [https://doi.org/10.1016/s0022-1694\(03\)00168-9](https://doi.org/10.1016/s0022-1694(03)00168-9)
- Liang, X., Guo, J. Z., & Leung, L. R. (2004). Assessment of the effects of spatial resolutions on daily water flux simulations. *Journal of Hydrology*, *298*(1–4), 287–310. <https://doi.org/10.1016/j.jhydrol.2003.07.007>
- Liang, X., Lettenmaier, D. P., & Wood, E. F. (1996). One-dimensional statistical dynamic representation of subgrid spatial variability of precipitation in the two-layer variable infiltration capacity model. *Journal of Geophysical Research*, *101*(D16), 21403–21422. <https://doi.org/10.1029/96jd01448>
- Liang, X., Lettenmaier, D. P., Wood, E. F., & Burges, S. J. (1994). A simple hydrologically based model of land surface water and energy fluxes for general circulation models. *Journal of Geophysical Research*, *99*(D7), 14415–14428. <https://doi.org/10.1029/94jd00483>
- Liang, X., Wood, E. F., & Lettenmaier, D. P. (1996). Surface soil moisture parameterization of the VIC-2L model: Evaluation and modification. *Global and Planetary Change*, *13*(1–4), 195–206. [https://doi.org/10.1016/0921-8181\(95\)00046-1](https://doi.org/10.1016/0921-8181(95)00046-1)
- Liang, X., Wood, E. F., & Lettenmaier, D. P. (1999). Modeling ground heat flux in land surface parameterization schemes. *Journal of Geophysical Research: Atmospheres*, *104*(D8), 9581–9600. <https://doi.org/10.1029/98JD02307>
- Liang, X., & Xie, Z. (2001). A new surface runoff parameterization with subgrid-scale soil heterogeneity for land surface models. *Advances in Water Resources*, *24*(9–10), 1173–1193. [https://doi.org/10.1016/S0309-1708\(01\)00032-X](https://doi.org/10.1016/S0309-1708(01)00032-X)
- Liang, X., Xie, Z., & Huang, M. (2003). A new parameterization for surface and groundwater interactions and its impact on water budgets with the variable infiltration capacity (VIC) land surface model. *Journal of Geophysical Research*, *108*(D16), 8613–8629. <https://doi.org/10.1029/2002jd003090>
- Maalim, F. K., Melesse, A. M., Belmont, P., & Gran, K. B. (2013). Modeling the impact of land use changes on runoff and sediment yield in the Le Sueur watershed, Minnesota using GeoWEPP. *Catena*, *107*, 35–45. <https://doi.org/10.1016/j.catena.2013.03.004>
- Mao, D., Cherkauer, K. A., & Flanagan, D. C. (2010). Development of a coupled soil erosion and large-scale hydrology modeling system. *Water Resources Research*, *46*(8), W08543. <https://doi.org/10.1029/2009wr008268>
- Matsushi, Y., & Matsukura, Y. (2006). Cohesion of unsaturated residual soils as a function of volumetric water content. *Bulletin of Engineering Geology and the Environment*, *65*(4), 449–455. <https://doi.org/10.1007/s10064-005-0035-9>
- Maurer, E., Wood, A., Adam, J., Lettenmaier, D., & Nijssen, B. (2002). A long-term hydrologically based dataset of land surface fluxes and states for the conterminous United States. *Journal of Climate*, *15*(22), 3237–3251. [https://doi.org/10.1175/1520-0442\(2002\)015<3237:althbd>2.0.co;2](https://doi.org/10.1175/1520-0442(2002)015<3237:althbd>2.0.co;2)
- Merritt, W. S., Letcher, R. A., & Jakeman, A. J. (2003). A review of erosion and sediment transport models. *Environmental Modelling and Software*, *18*(8–9), 761–799. [https://doi.org/10.1016/s1364-8152\(03\)00078-1](https://doi.org/10.1016/s1364-8152(03)00078-1)
- Miller, M. E., MacDonald, L. H., Robichaud, P. R., & Elliot, W. J. (2012). Predicting post-fire hillslope erosion in forest lands of the western United States. *International Journal of Wildland Fire*, *20*(8), 982–999. <https://doi.org/10.1071/wf09142>
- Morgan, R. P. C., & Nearing, M. A. (2011). *Handbook of erosion modelling*. Wiley Online Library. <https://doi.org/10.1002/9781444328455>
- Morgan, R. P. C., Quinton, J., Smith, R., Govers, G., Poesen, J., Auerswald, K., et al. (1998). The European soil erosion model (EUROSEM): A dynamic approach for predicting sediment transport from fields and small catchments. *Earth Surface Processes and Landforms*, *23*(6), 527–544. [https://doi.org/10.1002/\(sici\)1096-9837\(199806\)23:6<527::aid-esp868>3.0.co;2-5](https://doi.org/10.1002/(sici)1096-9837(199806)23:6<527::aid-esp868>3.0.co;2-5)
- Morris, M. D. (1991). Factorial sampling plans for preliminary computational experiments. *Technometrics*, *33*(2), 161–174. <https://doi.org/10.2307/1269043>
- Mouazen, A. M., Ramon, H., & Baerdemaeker, J. D. (2002). SW—Soil and water: Effects of bulk density and moisture content on selected mechanical properties of sandy loam soil. *Biosystems Engineering*, *83*(2), 217–224. <https://doi.org/10.1006/bioe.2002.0103>
- Nash, J. E., & Sutcliffe, J. V. (1970). River flow forecasting through conceptual models part I—A discussion of principles. *Journal of Hydrology*, *10*(3), 282–290. [https://doi.org/10.1016/0022-1694\(70\)90255-6](https://doi.org/10.1016/0022-1694(70)90255-6)
- Neitsch, S. L., Arnold, J. G., & Williams, J. R. (2011). *Soil and water assessment tool theoretical documentation (version 2009)* Texas Water Resources Institute Technical Report No. 406. Texas A&M University System.
- Nijssen, B., Schnur, R., & Lettenmaier, D. P. (2001). Global retrospective estimation of soil moisture using the variable infiltration capacity land surface model, 1980–93. *Journal of Climate*, *14*(8), 1790–1808. [https://doi.org/10.1175/1520-0442\(2001\)014<1790:greosm>2.0.co;2](https://doi.org/10.1175/1520-0442(2001)014<1790:greosm>2.0.co;2)
- Nilson, T. (1971). A theoretical analysis of the frequency of gaps in plant stands. *Agricultural Meteorology*, *8*, 25–38. [https://doi.org/10.1016/0002-1571\(71\)90092-6](https://doi.org/10.1016/0002-1571(71)90092-6)
- O'Callaghan, J. F., & Mark, D. M. (1984). The extraction of drainage networks from digital elevation data. *Computer Vision, Graphics, and Image Processing*, *28*(3), 323–344. [https://doi.org/10.1016/s0734-189x\(84\)80011-0](https://doi.org/10.1016/s0734-189x(84)80011-0)
- Parks, S., Mitchell, J., & Scarborough, J. (1982). Soil erosion simulation on small watersheds: A modified ANSWERS model. *Transactions of the American Society of Agricultural and Biological Engineers*, *25*(6), 1581–1588. <https://doi.org/10.13031/2013.33771>
- Pelletier, J. D. (2012). A spatially distributed model for the long-term suspended sediment discharge and delivery ratio of drainage basins. *Journal of Geophysical Research*, *117*(F2), F02028. <https://doi.org/10.1029/2011jf002129>
- Post, D., Waterhouse, J., Grundy, M., & Cook, F. (2007). The past, present and future of sediment and nutrient modelling in GBR Catchments. In *CSIRO, water for a healthy country national research flagship*.
- Prentice, I. C., Liang, X., Medlyn, B. E., & Wang, Y. P. (2015). Reliable, robust and realistic: The three R's of next-generation land-surface modelling. *Atmospheric Chemistry and Physics*, *15*(10), 5987–6005. <https://doi.org/10.5194/acp-15-5987-2015>

- Rodríguez-Iturbe, I., & Mejía, J. M. (1974). The design of rainfall networks in time and space. *Water Resources Research*, *10*(4), 713–728. <https://doi.org/10.1029/wr010i004p00713>
- Smith, R., Goodrich, D., & Quinton, J. N. (1995). Dynamic, distributed simulation of watershed erosion: The KINEROS2 and EUROSEM models. *Journal of Soil and Water Conservation*, *50*(5), 517–520.
- Stewart, J. R., Livneh, B., Kasprzyk, J. R., Rajagopalan, B., Minear, J. T., & Raseman, W. J. (2017). A multialgorithm approach to land surface modeling of suspended sediment in the Colorado front range. *Journal of Advances in Modeling Earth Systems*, *9*(7), 2526–2544. <https://doi.org/10.1002/2017MS001120>
- Sun, R., Hernandez, F., Liang, X., & Yuan, H. (2020). A calibration framework for high-resolution hydrological models using a multiresolution and heterogeneous strategy. *Water Resources Research*, *56*(8), e2019WR026541. <https://doi.org/10.1029/2019WR026541>
- Tan, Z., Leung, L. R., Li, H., Tesfa, T., Vanmaercke, M., Poesen, J., et al. (2017). A global data analysis for representing sediment and particulate organic carbon yield in Earth system models. *Water Resources Research*, *53*(12), 10674–10700. <https://doi.org/10.1002/2017WR020806>
- Tan, Z., Leung, L. R., Li, H.-Y., & Tesfa, T. (2018). Modeling sediment yield in land surface and Earth system models: Model comparison, development, and evaluation. *Journal of Advances in Modeling Earth Systems*, *10*(9), 2192–2213. <https://doi.org/10.1029/2017ms001270>
- Torri, D., Sfalanga, M., & Del Sette, M. (1987). Splash detachment: Runoff depth and soil cohesion. *Catena*, *14*(1–3), 149–155. [https://doi.org/10.1016/s0341-8162\(87\)80013-9](https://doi.org/10.1016/s0341-8162(87)80013-9)
- van Dijk, A. I. J. M., Meesters, A. G. C. A., Schellekens, J., & Bruijnzeel, L. A. (2005). A two-parameter exponential rainfall depth-intensity distribution applied to runoff and erosion modelling. *Journal of Hydrology*, *300*(1–4), 155–171. <https://doi.org/10.1016/j.jhydrol.2004.06.001>
- van Griensven, A., Meixner, T., Grunwald, S., Bishop, T., Diluzio, M., & Srinivasan, R. (2006). A global sensitivity analysis tool for the parameters of multi-variable catchment models. *Journal of Hydrology*, *324*(1–4), 10–23. <https://doi.org/10.1016/j.jhydrol.2005.09.008>
- Wen, Z., Liang, X., & Yang, S. (2012). A new multiscale routing framework and its evaluation for land surface modeling applications. *Water Resources Research*, *48*(8), W08528. <https://doi.org/10.1029/2011wr011337>
- Wuddivira, M. N., Stone, R. J., & Ekwue, E. I. (2009). Clay, organic matter, and wetting effects on splash detachment and aggregate breakdown under intense rainfall. *Soil Science Society of America Journal*, *73*(1), 226–232. <https://doi.org/10.2136/sssaj2008.0053>
- Xie, X., Liang, S., Yao, Y., Jia, K., Meng, S., & Li, J. (2015). Detection and attribution of changes in hydrological cycle over the Three-North region of China: Climate change versus afforestation effect. *Agricultural and Forest Meteorology*, *203*(0), 74–87. <https://doi.org/10.1016/j.agrformet.2015.01.003>
- Xie, X., & Liang, X. (2024). A physically-based soil erosion and sediment transport model (VIC-SED) for large-scale applications: Program code and cases. *Zenodo*. <https://doi.org/10.5281/zenodo.12782448>
- Yu, X., Xie, X., & Meng, S. (2017). Modeling the responses of water and sediment discharge to climate change in the upper Yellow River basin, China. *Journal of Hydrologic Engineering*, *22*(12). [https://doi.org/10.1061/\(asce\)jhe.1943-5584.0001590](https://doi.org/10.1061/(asce)jhe.1943-5584.0001590)
- Zhang, H., Lauerwald, R., Regnier, P., Ciais, P., Yuan, W., Naipal, V., et al. (2020). Simulating erosion-induced soil and carbon delivery from uplands to rivers in a global land surface model. *Journal of Advances in Modeling Earth Systems*, *12*(11), e2020MS002121. <https://doi.org/10.1029/2020ms002121>